



Root Exudates Alter the Expression of Diverse Metabolic, Transport, Regulatory, and Stress Response Genes in Rhizosphere *Pseudomonas*

OPEN ACCESS

Edited by:

Barbara Pivato,
Institut National de Recherche pour
l'agriculture, l'alimentation et
l'environnement (INRAE), France

Reviewed by:

Cara Helene Haney,
The University of British Columbia,
Canada
Xingang Zhou,
Northeast Agricultural University,
China

*Correspondence:

Dmitri V. Mavrodi
dmitri.mavrodi@usm.edu
Alex S. Flynt
alex.flynt@usm.edu

†These authors have contributed
equally to this work

Specialty section:

This article was submitted to
Microbe and Virus Interactions with
Plants,
a section of the journal
Frontiers in Microbiology

Received: 09 January 2021

Accepted: 08 March 2021

Published: 14 April 2021

Citation:

Mavrodi OV, McWilliams JR,
Peter JO, Berim A, Hassan KA,
Elbourne LDH, LeTourneau MK,
Gang DR, Paulsen IT, Weller DM,
Thomashow LS, Flynt AS and
Mavrodi DV (2021) Root Exudates
Alter the Expression of Diverse
Metabolic, Transport, Regulatory,
and Stress Response Genes
in Rhizosphere *Pseudomonas*.
Front. Microbiol. 12:651282.
doi: 10.3389/fmicb.2021.651282

Olga V. Mavrodi^{1†}, Janiece R. McWilliams^{1†}, Jacob O. Peter¹, Anna Berim²,
Karl A. Hassan³, Liam D. H. Elbourne⁴, Melissa K. LeTourneau⁵, David R. Gang²,
Ian T. Paulsen⁴, David M. Weller⁵, Linda S. Thomashow⁵, Alex S. Flynt^{1*} and
Dmitri V. Mavrodi^{1*}

¹ School of Biological, Environmental, and Earth Sciences, The University of Southern Mississippi, Hattiesburg, MS, United States, ² Institute of Biological Chemistry, Washington State University, Pullman, WA, United States, ³ School of Environmental and Life Sciences, The University of Newcastle, Callaghan, NSW, Australia, ⁴ Department of Molecular Sciences, Macquarie University, Sydney, NSW, Australia, ⁵ USDA Agricultural Research Service, Wheat Health, Genetics and Quality Research Unit, Pullman, WA, United States

Plants live in association with microorganisms that positively influence plant development, vigor, and fitness in response to pathogens and abiotic stressors. The bulk of the plant microbiome is concentrated belowground at the plant root-soil interface. Plant roots secrete carbon-rich rhizodeposits containing primary and secondary low molecular weight metabolites, lysates, and mucilages. These exudates provide nutrients for soil microorganisms and modulate their affinity to host plants, but molecular details of this process are largely unresolved. We addressed this gap by focusing on the molecular dialog between eight well-characterized beneficial strains of the *Pseudomonas fluorescens* group and *Brachypodium distachyon*, a model for economically important food, feed, forage, and biomass crops of the grass family. We collected and analyzed root exudates of *B. distachyon* and demonstrated the presence of multiple carbohydrates, amino acids, organic acids, and phenolic compounds. The subsequent screening of bacteria by Biolog Phenotype MicroArrays revealed that many of these metabolites provide carbon and energy for the *Pseudomonas* strains. RNA-seq profiling of bacterial cultures amended with root exudates revealed changes in the expression of genes encoding numerous catabolic and anabolic enzymes, transporters, transcriptional regulators, stress response, and conserved hypothetical proteins. Almost half of the differentially expressed genes mapped to the variable part of the strains' pangenome, reflecting the importance of the variable gene content in the adaptation of *P. fluorescens* to the rhizosphere lifestyle. Our results collectively reveal the diversity of cellular pathways and physiological responses underlying the establishment of mutualistic interactions between these beneficial rhizobacteria and their plant hosts.

Keywords: *Pseudomonas*, *Brachypodium*, rhizosphere, root exudates, transcriptome

INTRODUCTION

Plants are meta-organisms or holobionts that rely in part on their microbiome for specific functions and traits. The ability of the plant microbiome to influence plant development, vigor, health, and fitness in response to abiotic stressors associated with global climate change is documented by numerous studies (Lugtenberg and Kamilova, 2009). There is mounting evidence that plants actively recruit beneficial microbiomes, but many aspects of this process are still very much a black box (Reinhold-Hurek et al., 2015). The foundation for the differential affinity of rhizobacteria toward host plants is built upon complex chemical cross talk between microorganisms and plant roots. Up to 40% of photosynthetically fixed carbon is released by plant roots in the form of exudates and secretions, lysates, and mucilages (Curl and Truelove, 1986; Lynch, 1990; Whipps, 1990; Badri and Vivanco, 2009). The release of these compounds is actively controlled in response to environmental stimuli, and the composition of root exudates varies greatly according to plant species and physiological condition (Lynch, 1990; Nguyen, 2003; Phillips et al., 2004; De-la-Pena et al., 2008). The presence and composition of exudates strongly impact soil microorganisms, which is consistent with the idea that plants actively select and shape their root microbiota (Zolla et al., 2013).

Primary root exudates include simple and complex sugars, amino acids, polypeptides and proteins, organic, aliphatic and fatty acids, sterols, and phenolics (Nguyen, 2003; Badri and Vivanco, 2009; Badri et al., 2009). These compounds serve as carbon and energy sources for rhizobacteria, and the presence of the intact corresponding catabolic pathways is essential for competitive colonization of roots and disease suppression (Lugtenberg et al., 2001; Kamilova et al., 2005; Lugtenberg and Kamilova, 2009). Root exudates also contain numerous signal molecules and secondary metabolites, the significance of which is only now emerging (Walker et al., 2003; Bais et al., 2005, 2006). A handful of analyses of plant-induced gene expression by transcriptional profiling *in vitro* (Mark et al., 2005) or in the rhizosphere (Silby and Levy, 2004; Ramos-Gonzalez et al., 2005; Matilla et al., 2007; Barret et al., 2009) have identified multiple genes that are differentially regulated by exposure to roots or root exudates. Bacterial pathways expressed during rhizosphere colonization control utilization of plant-derived metabolites (Simons et al., 1996, 1997; Camacho-Carvajal, 2001; Lugtenberg and Kamilova, 2009), motility and chemotaxis (de Weert et al., 2002; Lugtenberg and Kamilova, 2009), phase variation (Dekkers et al., 1998; Sanchez-Contreras et al., 2002; van den Broek et al., 2005), outer membrane integrity (de Weert et al., 2006; Lugtenberg and Kamilova, 2009), and the ability to sequester limiting resources (Raaijmakers et al., 1995) and resist environmental stresses (Sarniguet et al., 1995; Miller and Wood, 1996; van Veen et al., 1997; Schnider-Keel et al., 2001). In its spatial and temporal properties, root colonization resembles biofilm formation, and biofilm-related pathways also have been implicated in adhesion to seeds and roots and rhizosphere colonization (Espinosa-Urgel et al., 2000; Hinsia et al., 2003; Yousef-Coronado et al., 2008; Fuqua, 2010; Martinez-Gil et al., 2010; Nielsen et al., 2011; Zboralski and Fillion, 2020). Finally,

root exudates strongly affect the expression of diverse plant growth promotion and biocontrol genes (Vacheron et al., 2013). Over the past decade, the genomes of numerous rhizosphere strains have been sequenced and analyzed, but functional genomics studies of rhizosphere competence lag behind the availability of sequence data.

This study explored the molecular dialog between the model host plant *Brachypodium distachyon* and several well-characterized rhizosphere strains of the *Pseudomonas fluorescens* group. *Brachypodium* is a small annual grass originating in semi-arid regions of the Middle East that has emerged as a prime model for economically important food, feed, forage, and biomass crops of the grass family (Bevan et al., 2010; Schwartz et al., 2010; Brkljacic et al., 2011; Hong et al., 2011; Tyler et al., 2014). The biology, extensive collection of resources, and research tools make *B. distachyon* an attractive model to investigate interactions between plants and root-associated microbes. Pseudomonads are ubiquitous Gram-negative γ -proteobacteria that colonize eukaryotic hosts and include both commensals and economically important pathogens of plants and animals (Moore et al., 2006; Schroth et al., 2006; Yahr and Parsek, 2006). The genus *Pseudomonas* currently comprises > 100 named species that have been separated based on multilocus sequence analysis into 14 species groups (Garrido-Sanz et al., 2016; Hesse et al., 2018). The *P. fluorescens* group is the most diverse regarding both the genetic distances within it, the number of species and the large pangenome that makes up > 50% of the pangenome of the genus as a whole (Loper et al., 2012). The group also encompasses an unusually high proportion of strains that inhabit the plant rhizosphere and possess plant growth promoting and biocontrol properties. Naylor et al. (2017) profiled bacterial communities associated with root tissues and rhizosphere of 18 different plant species of the *Poaceae* family. That study identified *Pseudomonas* among taxa constituting the core grass root microbiome and demonstrated that these bacteria were enriched in C3 plants, including wheat, rye, barley, oat, and *Brachypodium*. We confirmed the capacity of *B. distachyon* Bd21 to serve as a host for rhizobacteria of the *P. fluorescens* group in preliminary greenhouse assays with biocontrol strains *P. synxantha* 2-79, *P. brassicacearum* Q8r1-96, and *P. protegens* Pf-5. Results of these experiments revealed that all strains successfully established and colonized the roots of *Brachypodium* (**Supplementary Table 1**).

In this study, we focused on eight well-studied strains of the *P. fluorescens* complex that are supported by years of studies, numerous refereed publications, and high-quality genome sequences. By profiling transcriptomes of these strains during growth in root exudates of *B. distachyon*, we revealed the diversity of cellular pathways and physiological responses that underlie the establishment of mutualistic interactions between beneficial rhizobacteria and the host plant. Our results also confirmed that root exudates contain carbohydrates, amino acids, organic acids, and phenolics that serve as carbon and energy sources for rhizobacteria. The root exudates also contained osmoprotectants that may help microorganisms to persist in the rhizosphere of drought-stressed plants. The diversity of microbial genes perturbed by root exudates reflects the importance of

the variable genome in adaptation of individual strains of *Pseudomonas* to the rhizosphere lifestyle.

MATERIALS AND METHODS

Bacterial Strains Used in the Study

The eight *Pseudomonas* strains used for this study are *P. synxantha* 2-79 (Thomashow and Weller, 1988), *P. fluorescens* SBW25 (Silby et al., 2009), *Pseudomonas* sp. R1-43-08 (Parejko et al., 2012), *P. brassicacearum* Q8r1-96 (Raaijmakers and Weller, 1998), *P. fluorescens* Q2-87 (Bangera and Thomashow, 1996), *P. chlororaphis* 30-84 (Thomashow et al., 1990), *P. fluorescens* Pf0-1 (Silby et al., 2009), and *P. protegens* Pf-5 (Howell and Stipanovic, 1980). The selected organisms have been studied extensively for their role in biological control and plant growth promotion (**Supplementary Table 2**). The strains were maintained in the laboratory as frozen stocks (-80°C) and routinely cultured in King's medium B (King et al., 1954) or 21C medium, which contained (per 1 L): 1.0 g of NH_4Cl , 3.5 g of $\text{Na}_2\text{HPO}_4 \cdot 2\text{H}_2\text{O}$, 2.8 g of KH_2PO_4 , 3.0 g of glucose, and 20 ml of a microelement solution (Smibert and Kreig, 1994; Halverson and Firestone, 2000).

Propagation of Plants and Collection of Root Exudates

B. distachyon Bd21 was established from seed material obtained from the USDA-ARS Plant Germplasm Introduction and Testing Research Unit (Pullman, WA, United States). *Brachypodium* seeds were imbibed for 3 days at 4°C and sown in 7×7 cm pots filled with Sunshine Potting Mix #4 (Sun Gro Horticulture, Agawam, MA, United States). Plants were grown in an IR-89X (Percival Scientific, Perry, IA, United States) controlled environment chamber retrofitted with 6500K and 3000K T5 54W grow lights (Spectralux) under a 20-h light, $24^{\circ}\text{C}/4$ -h dark, 18°C cycle. Plants were watered and fertilized with Jack's professional water-soluble fertilizer (20:20:20) (JR Peters, Allentown, PA, United States). After 12 weeks and plant senescence, seeds were collected, processed, and stored under desiccant and dark conditions at room temperature.

To collect root exudates, seeds of *B. distachyon* Bd21 were surface-sterilized, pregerminated, and placed in sterile 1 L wide-mouth glass jars containing 113 g of 6-mm glass beads and 25 ml distilled water. Jars were covered with vented caps and plants were grown hydroponically in an environmental controlled growth chamber under conditions described above. After 6 days, root exudates were extracted from individual jars and their sterility was confirmed by spotting on nutrient agar. Multiple batches of root exudates were collected, filtered ($0.22 \mu\text{m}$), aliquoted in Falcon tubes (10 ml), lyophilized, and stored at -80°C .

Metabolomic Profiling of Root Exudates

Exudates were analyzed for primary metabolites at the Murdock Metabolomics Laboratory at Washington State University (Pullman, WA, United States). Freeze-dried residues were

suspended in 500 μl 50% aqueous acetonitrile and clarified by centrifugation for 20 min at $21,000 \times g$ and 4°C . The liquid chromatography mass spectrometry analysis was conducted with a Synapt G2-S quadrupole-ion mobility spectrometry-time of flight mass spectrometer system equipped with an acquity ultra-performance liquid chromatograph (UPLC) and an acquity photodiode array detector (all from Waters, Milford, MA, United States). The exudate metabolites were separated on a SeQuant ZIC-pHILIC HPLC column (2.1×100 mm, $3 \mu\text{m}$) (Millipore Sigma, Burlington, MA, United States) using acetonitrile with 0.1% formic acid as solvent B and water with 0.1% formic acid as solvent A at a flow rate of $400 \mu\text{l min}^{-1}$ and the following linear gradient extending over 14 min: 0 min, 80% B; 4 min, 80% B; 6 min: 10% B; 7.5 min, 10% B; 10 min, 80% B; and 14 min, 80% B. Mass spectra were collected in positive ion mode over a range of m/z 50–1,200 with a scan time of 0.2 s. The Q-TOF-MS source was at 3.0 kV and 120°C ; the sampling cone at 40 V, desolvation temperature was 250°C ; cone gas and desolvation gas flow were at 0 and 850 L h^{-1} , respectively. Leucine enkephalin was used for post-acquisition mass correction. Target compounds were visualized using selected ion chromatograms at 0.05 Da window width. The compound identification was based on comparison of chromatographic behavior and accurate masses to those of authentic standards.

For gas chromatography, derivatization was carried out using a modification of the procedure of Lee and Fiehn (2008). The freeze-dried residues were suspended in 950 μl aqueous methanol (84%, v/v) and clarified by centrifugation for 15 min at $21,000 \times g$ at 4°C . The supernatants were spiked with 1 μg of the internal standard salicylic acid- d_6 (C/D/N Isotopes, Quebec, Canada) and dried *in vacuo*. The dry residues were suspended in 10 μl of *O*-methoxylamine hydrochloride (30 mg ml^{-1} in anhydrous pyridine, both from Millipore Sigma) and incubated while mixing (1,000 RPM) for 90 min at 30°C . Subsequently, samples were derivatized with 90 μl of MSTFA with 1% TMCS (Thermo Fisher Scientific, Waltham, MA, United States) for 30 min at 37°C . Gas chromatography-mass spectroscopy analysis was performed using a Pegasus 4D time-of-flight mass spectrometer (LECO, Saint Joseph MI) equipped with a MPS2 autosampler (Gerstel, Linticum, MD) and a 7890A oven (Agilent Technologies, Santa Clara, CA, United States). The derivatization products were separated on a 30-m, 0.25 mm i.d., $0.25 \mu\text{m d}_f$ Rxi-5Sil column (Restek, Bellefonte, PA, United States) with an IntegraGuard precolumn using ultrapure He at a constant flow of 0.9 ml min^{-1} as carrier gas. The linear thermal gradient started with a 1-min hold at 70°C , followed by a ramp to 300°C at $10^{\circ}\text{C min}^{-1}$. The final temperature was held for 5 min prior to returning to initial conditions. Mass spectra were collected at 17 spectra s^{-1} . Peak identification was conducted using the Fiehn primary metabolite library (Kind et al., 2009) and an identity score cutoff of 700. Additionally, authentic standards for a number of primary metabolites were analyzed under identical conditions and the data used to compare the chromatographic behavior. Peak alignment and spectrum comparisons were carried out using the Statistical Compare feature of ChromaTOF software (LECO).

Isolation of RNA From Bacteria Cultured in Root Exudates and RNA-Seq

The strains were pregrown overnight at 25°C on 21C-glucose agar and then subcultured into 96-well microplates containing liquid 21C-glucose medium amended with *Brachypodium* exudates. The liquid medium was prepared by dissolving the lyophilized root exudate material in an appropriate volume of 21C-glucose medium to concentrate root exudates 20-fold. The growth medium was sterilized by passing it through a 0.22- μ m membrane filter. The control cultures were grown under identical conditions in the absence of exudates. All treatments were inoculated at OD₆₀₀ of 0.1 and incubated for 20 to 22 h until cultures entered late-exponential growth phase at 25°C in an atmosphere of 15% oxygen [created by a ProOx P110 oxygen controller (BioSpherix, Parish, NY, United States) with a hypoxia C-chamber]. The cells were stabilized by the addition RNAprotect reagent (QIAGEN, Germantown, MD, United States) and total RNA was purified using a RNeasy Protect Bacteria Mini Kit (QIAGEN) from three biological replicates of each strain cultured under control conditions and in exudates. The quality assessment of the extracted RNA samples was performed with a NanoDrop One^C Spectrophotometer (Thermo Fisher Scientific) and a 2100 Bioanalyzer (Agilent Technologies) and revealed A₂₆₀/A₂₈₀ and A₂₆₀/A₂₃₀ values of > 2.0 and a mean RNA integrity numbers (RIN) value of > 9.2.

Three biological replicates of RNA samples were shipped on dry ice to the DOE Joint Genome Institute (Walnut Creek, CA, United States), where rRNA was depleted and stranded RNA-Seq libraries were prepared, quantified by qPCR and sequenced using a HiSeq 2500 instrument (Illumina). The fastq file reads were filtered and processed with BBDuk¹ to remove reads that contained 1 or more “N” bases, had an average quality score across the read less than 10 or had a minimum length \leq 51 bp or 33% of the full read length. Reads mapped with BBDuk (see text footnote 2) to masked human, cat, dog, and mouse references at 93% identity were removed. Another category of removed sequences matched RNA spike-in, PhiX, common microbial contaminants, and ribosomal RNAs. The processed reads from each library were aligned to the reference genome using BBDuk with only unique mappings allowed (BAMs/directory). If a read mapped to more than one location it was ignored. featureCounts (Liao et al., 2014) was used to generate raw gene counts, which were normalized to adjust for the length of each gene and total number of reads mapped for each library. The normalization formula used: $n = [r/(l/1,000)]/(t/1,000,000)$, where n = normalized read count for gene (G) for library (L); r = raw read count for gene G for library L ; l = gene G length; and t = total reads mapped for library L . Raw gene counts were used to evaluate the level of correlation between biological samples using Pearson's correlation.

Bioinformatic Analysis

Count tables generated by the JGI RNA-Seq pipeline were input into DESeq2 (Love et al., 2014) to normalize and determine

differential expression. Statistical significance was established through DESeq2 by using three biological replicates for control and root exudate conditions. Scatterplots were generated from the DESeq2 data table outputs using ggplot2. Genes differentially expressed between control and root exudate samples (\log_2 fold-changes $-2 \geq$ to ≤ 2 , adjusted p value ≤ 0.05) were used in downstream analysis. The core genome and pangenome for the *Pseudomonas* strains used in this study were computed using the OthoMCL v.2.0, Species Tree Builder v.2.2.0, and Phylogenetic Pangenome Accumulation v1.4.0 apps implemented in the U.S. Department of Energy Systems Biology Knowledgebase (KBase) (Arkin et al., 2018). Additional comparisons were conducted with the PGAweb pangenome analysis pipeline (Chen et al., 2018). Differentially expressed genes were assigned to core, non-core, and singleton parts of each strain's proteome by BLASTp with an E value cutoff of $e-06$, identity of 40% and coverage of 60%. Functional annotation of differentially expressed genes was carried out with the Blast2GO (Conesa and Gotz, 2008) and visualized in WEGO 2.0 (Ye et al., 2018). Additional manual curation was performed using tools implemented in the Integrated Microbial Genomes (IMG) database (Markowitz et al., 2012), Pseudomonas Genome Database (Winsor et al., 2009), Kyoto Encyclopedia of Genes and Genomes (KEGG) (Kanehisa et al., 2008), and Geneious 10.2.3 (Biomatters, Auckland, New Zealand). Metabolic functions encoded by the differentially expressed genes were mapped using iPath 3.0 (Darzi et al., 2018). Phylogenetic analyses were carried out by building multiple sequence alignments with MAFFT v7.222 (Katoh and Standley, 2013) and inferring neighbor-joining (NJ) phylogenies with Geneious Tree Builder. The resultant phylogenetic trees were visualized with iTOL (Letunic and Bork, 2016). Reproducibility of clades within the inferred NJ trees was assessed by bootstrap resampling with 1,000 replicates.

Characterization of Carbon Source Utilization With Biolog Phenotype Microarrays

The utilization of carbon sources was analyzed using Phenotype MicroArrays (Biolog, Hayward, CA, United States) as follows. The bacteria were cultured overnight on Luria-Bertani agar at 25°C, after which cells were harvested and suspended in inoculating fluid (IF-0). The transmittance of the suspension was adjusted to 42% using a Biolog turbidimeter. The cell suspension was mixed with IF-0 containing Dye Mix A (Biolog) to achieve a final transmittance of 85%. One hundred microliter aliquots of the adjusted cell suspension were inoculated into PM01 and PM02A plates, which were then incubated in an OmniLog Phenotype MicroArray System (Biolog) at 25°C for 48 h. The formation of formazan was recorded at 15 min intervals, and data were analyzed using OmniLog Parametric Analysis software v1.20.02 (Biolog). Relative growth of the studied strains was normalized to growth on D-glucose and visualized using Heatmapper (Babicki et al., 2016).

¹<https://sourceforge.net/projects/bbdmap/>

Data Availability

Sequences generated in this project were deposited under NCBI BioProject accession numbers PRJNA439743 through PRJNA439790.

RESULTS

Metabolomic Profiling of Root Exudates of *B. distachyon*

Metabolomics analysis of lyophilized root exudates revealed the presence of numerous plant metabolites, 86 of which were identified by matching their spectra to the LECO/Fiehn Metabolomics library (**Supplementary Table 3**). These metabolites included (i) carbohydrates and their derivatives (glucose, fructose, xylose, sucrose, trehalose, maltose, galactose, and others); (ii) sugar alcohols (β -mannosylglycerate, myo-inositol, galactinol, 2-deoxyerythritol, ribitol, threitol and cellobitol); (iii) amino acids and derivatives (glutamine, tyrosine, glutamic acid, asparagine, aspartic acid, valine, phenylalanine, isoleucine, glycine, serine, proline, leucine, tryptophan, cysteine, methionine, citrulline, and others); (iv) organic acids (aconitic, allantoic, γ -aminobutyric, azelaic, citric, fumaric, 2-furoic, D-glyceric, 3-hydroxypropionic, α -keto adipic, malic, methylmalonic, nicotinic, quinic, succinic, threonic); and (v) assorted metabolites including heterocyclic compounds, phenolics, and biogenic amines, etc (3-hydroxypyridine, maleimide, noradrenaline, 4-hydroxy-3-methoxybenzoate, 5-methoxytryptamine, uracil, aminomalonic acid, palmitic acid, and urea). Results of the analysis also revealed that root exudates of *B. distachyon* contain hydroxyectoine and the quaternary amine (QA) glycine betaine (**Supplementary Figure 1**).

Phylogenetic and Pangenome Analyses of *Pseudomonas* Strains Used in the Study

We used a set of phylogenetic markers suggested by Mulet et al. (2010) to investigate the relatedness of the eight strains used in this study to distinct lineages recognized within the *P. fluorescens* species complex. The multilocus sequence analysis based on the concatenated sequences of the housekeeping genes *rrs* (16S rRNA), *gyrB*, *rpoB*, and *rpoD* identified R1-43-08 (along with strains 2-79 and SBW25) as a member of the *P. fluorescens* subgroup (**Figure 1**). The rest of the strains clustered closely with four additional subgroups of the *P. fluorescens* complex, namely *P. corrugata* (strains Q2-87 and Q8r1-96), *P. koreensis* (Pf0-1), *P. protegens* (Pf-5), and *P. chlororaphis* (30–84). The genomes of the eight rhizosphere *Pseudomonas* strains varied in size by 1.43 megabase (ranging from 5.65 to 7.07 Mb) and contained between 5,166 and 6,363 protein-coding genes (**Figure 2A**). The shared gene content was characterized with OrthoMCL, which uses all-against-all BLASTp followed by the Markov Cluster algorithm to identify protein groups shared between the compared genomes, as well as groups representing species-specific gene expansion families (Li et al., 2003). The pangenome analysis revealed a core comprised of approximately 3,179 orthologs that were

shared among all strains and represented 50.0% to 61.5% of each predicted proteome (**Figures 2A,B**). The non-core pangenome contained genes shared by two or more (but not all) strains and contained between 1,482 and 2,080 orthologs, which corresponded to 28.7–36.3% of individual proteomes. The rest of the predicted protein-coding genes were strain-specific singletons that comprised 7.5% to 15.1% of the strain's predicted proteomes. In respect to divergence from the core genome, strain Pf-5 was found to possess the highest proportion of unique genes ($n = 949$) followed by 2-79 ($n = 887$). The entire pangenome of the *Pseudomonas* strains encompassed over 12,000 homolog and singleton gene families.

Further homolog family-based comparisons identified Q8r1-96 and R1-43-08 as the most distantly related strains, with 3349 shared homologs (**Supplementary Table 4A**). Q8r1-96 and Q2-87, which shared 4,489 homologs, were the most closely related strains. The partitioning of homolog gene families into the core, non-core, and singleton parts of the pangenome agreed with phylogenetic relationships of the strains deduced from the analysis of a selected subset of COGs (Clusters of Orthologous Groups) (**Figure 2C** and **Supplementary Tables 4B,C**). The COG-based phylogeny supported the multilocus sequence analysis and revealed that the eight *Pseudomonas* strains form three distinct clusters, the first of which contained 2-79, R1-30-84, and SBW25. The second cluster included Q8r1-96 and Q2-87, whereas the third encompassed strains 30-84, Pf-5, and Pf0-1.

Correlating the Composition of Root Exudates With Metabolic Profiles of *Pseudomonas* Strains

We used the Phenotype MicroArray PM1 and PM2 plates to profile the eight *Pseudomonas* strains for the utilization of 190 different carbon sources. Results of the analysis identified 90 compounds that supported growth and clustered by their intensities of utilization into three distinct groups (**Figure 3**). Group I was comprised of 30 highly metabolized carbon sources, which included several amino acids and intermediates of glycolysis, pyruvate metabolism, and citrate cycle. Approximately half of these compounds were catabolized by all eight strains, and included several organic acids (fumaric, citric, gluconic, malic, and pyroglutamic), amino acids (Glu, Asn, Gln, Asp, Pro, Ala, and γ -aminobutyric acid), carbohydrates (glucose, mannose, and mannitol), and the purine nucleoside inosine. Group II was composed of 44 chemically diverse carbon sources that were variably utilized by the strains. These compounds were carbohydrates, organic acids, amino acids, phenolics, and polyols, and included known compatible solutes and intermediates of metabolism of pentoses, galactose, starch, and sucrose. Group III encompassed the rest of the Phenotype MicroArray test panel and contained compounds that were not catabolized by the tested strains. Among several notable exceptions were α -hydroxyglutamic acid- γ -lactone, putrescine, and itaconic, citramalic, and succinamic acids, which supported the growth of strains 2-79, 30-84, Pf-5, and SBW25. We further matched the carbon metabolic profiles of the *Pseudomonas* strains against the list of plant-derived metabolites from the root exudates of

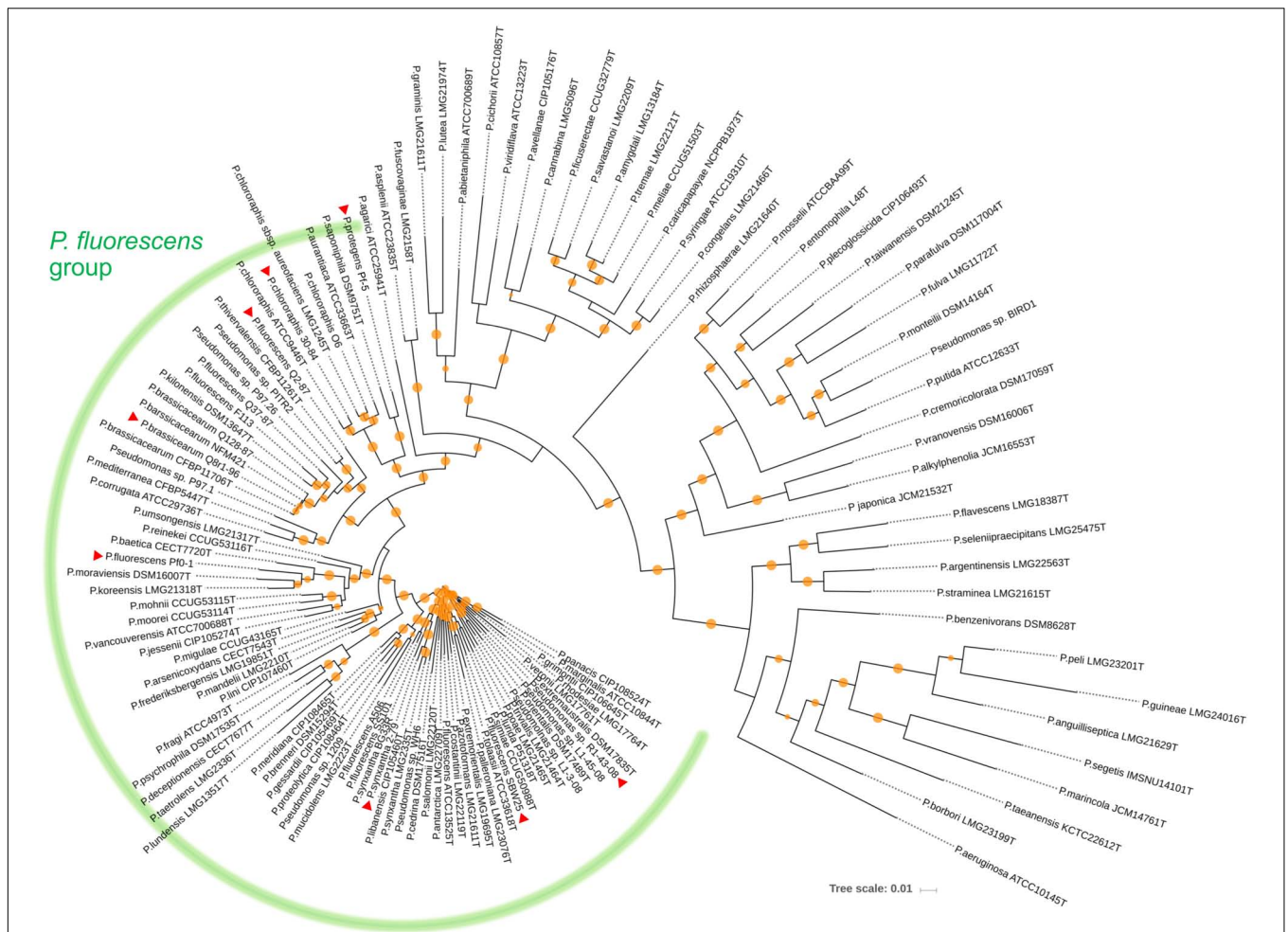
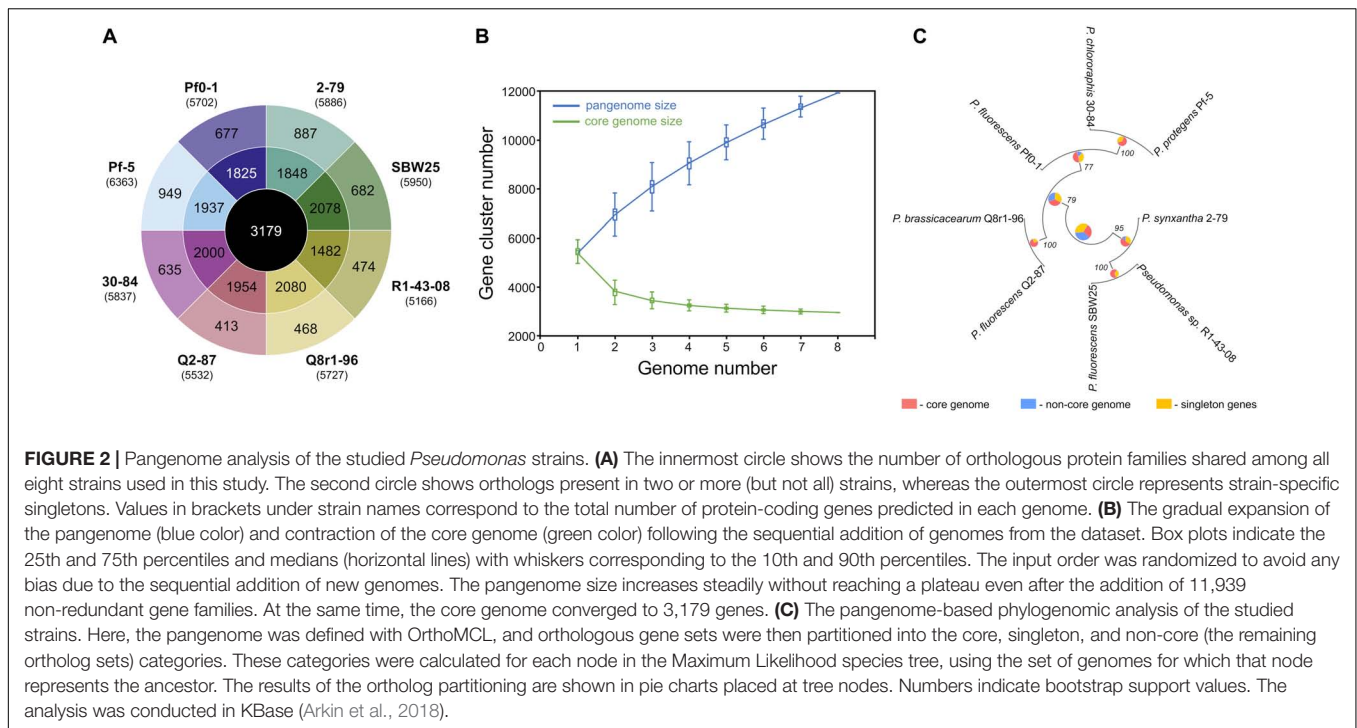


FIGURE 1 | Neighbor joining phylogeny showing the relationship of the eight strains used in this study (indicated by red triangles) to different species of the *P. fluorescens* complex. The phylogeny was established based on the concatenated sequences of the housekeeping genes *rrs* (16S rRNA), *gyrB* (subunit B of DNA gyrase), *rpoB* (β subunit of RNA polymerase), and *rpoD* (sigma 70 factor subunit of RNA polymerase). Distance matrices were calculated by the Jukes-Cantor method. Colored circles on tree nodes indicate bootstrap values (1,000 replicates) that vary between 60% (smallest circle) and 100% (largest circles).

B. distachyon Bd21. Interestingly, many carbon sources from the Phenotype MicroArray panel were also present in the root exudates of *B. distachyon* Bd21, and some of these compounds (glucose, mannose, galactose, fructose, γ -aminobutyric acid, aspartic acid, citric acid, malic acid, fumaric acid, quinic acid, alanine, glutamine, and glutamic acid) were catabolized by all strains used in this study, while others (e.g., xylose, trehalose, *m*-inositol) were actively utilized only by certain organisms (Figure 3). The comparison of catabolic profiles across the eight studied *Pseudomonas* strains revealed the presence of three distinct clusters. The first cluster contained strains Q8r1-96 and Q2-87, which consumed very similar sets of carbon sources, as well as strain Pf0-1. The second cluster was composed of 2-79, R1-43-08, SBW25, and 30-84, whereas the third cluster was represented by a single strain, Pf-5. The overall similarity of the catabolic profiles partially agreed with the separation of the strains into different subgroups of the *P. fluorescens* complex (see above).

Analysis of the RNA-seq Results

In order to understand the cellular responses of rhizosphere *Pseudomonas* to plant exometabolites, we analyzed the transcriptome changes in cultures grown in the presence of root exudates. Under field conditions, rhizobacteria colonize plant roots in the form of surface-attached microaerobic biofilms (Hojberg et al., 1999). To mimic these conditions, the eight *Pseudomonas* strains were grown statically at 72% air saturation in 21C-glucose medium amended with root exudates and then processed to extract total RNA (Supplementary Figure 2). A total of 995 million raw sequencing reads were generated from the RNA samples by using the Illumina HiSeq-2500 platform, averaging 20.7 million reads per sample. The removal of low-quality and rRNA sequences resulted in a total of 793 million filtered reads that were mapped onto the eight *Pseudomonas* genomes with a mean of 7.48 million mapped fragments per genome. The differentially abundant transcripts were identified by setting a *p* value of 0.05 (adjusted for multiple testing) and



the \log_2 fold-change (FC) threshold $\geq \pm 2.0$ (Figure 4 and Supplementary Tables 5–12). When compared with the control conditions, an average of 204 genes per strain were differentially expressed in the presence of root exudates, with the highest ($n = 425$) and lowest ($n = 112$) numbers observed, respectively, in SBW25 and Q2-87 (Figure 4). Overall, more genes were induced than repressed in response to exudates, but the actual numbers in each category varied substantially depending on the identity of the *Pseudomonas* strain. In most strains, the bulk of the differentially expressed genes was almost equally distributed between the core (mean, 48.2%) and non-core (mean, 45.8%) parts of the genome, whereas the strain-specific singleton genes constituted on average only 5.9% (Figure 4B). One notable exception was observed in Q8r1-96, where all differentially expressed genes belonged to the core (73.8%) and non-core (26.2%) parts of the genome. Another notable pattern was observed in R1-43-08, where the majority of genes affected by the presence of root exudate fell into the non-core category (56.3%). The highest proportion of differentially expressed singletons (11.3 and 10.4%, respectively) was identified in strains SBW25 and Pf-5.

We further explored how the identified differentially expressed genes were distributed across genomes of the eight studied rhizosphere strains. The pairwise BLASTp comparisons identified 2-79 and SBW25 as two strains that shared the highest number of genes ($n = 101$) induced or repressed in response to root exudates (Table 1). The second pair of strains with a significant number of similar differentially expressed genes ($n = 86$) was Q8r1-96 and Pf-5, which was followed by Pf0-1 and 30-84, which shared 56 differentially expressed genes. These patterns of shared genes were also observed when the results of the pairwise BLASTp comparisons were converted into a binary

gene presence/absence matrix, which was then subjected to cluster analysis using a UPGMA algorithm based on Sorensen's dissimilarity index or examined by non-metric multidimensional scaling (NMDS) (Figure 5).

The differentially expressed *Pseudomonas* genes were subjected to Blast2Go analysis and Gene Ontology (GO) annotation (Figure 6). Metabolic process, catalytic activity, and membrane were the most common annotation terms across the three primary GO term categories (i.e., biological process, molecular function, and cellular component). A total of 1,694 GO terms was assigned to 805 upregulated genes, with the majority of the GO terms related to molecular function (682, 40.3%), followed by biological process (669, 39.5%), and cellular component (343, 20.2%). In the 539 downregulated gene category, 1,101 GO terms were assigned to biological process (420, 38.1%), molecular function (417, 37.9%), and cellular component (264, 24.0%). Within biological process, metabolic process, cellular process, localization, response to stimulus, and regulation were over-represented. Within molecular function, the largest proportion was assigned to catalytic activity, binding, and transporter activity categories. Within cellular component, the majority were assigned to membrane, membrane part, cell, and cell part categories. Across the eight strains, 37–42% of differentially expressed genes had no Gene Ontology IDs and encoded various conserved hypothetical proteins.

Functional Classification of Shared Differentially Expressed Genes

The interrogation of RNA-seq data revealed multiple cellular pathways that were differentially regulated in bacterial cultures incubated with root exudates (Supplementary Figures 3, 4).

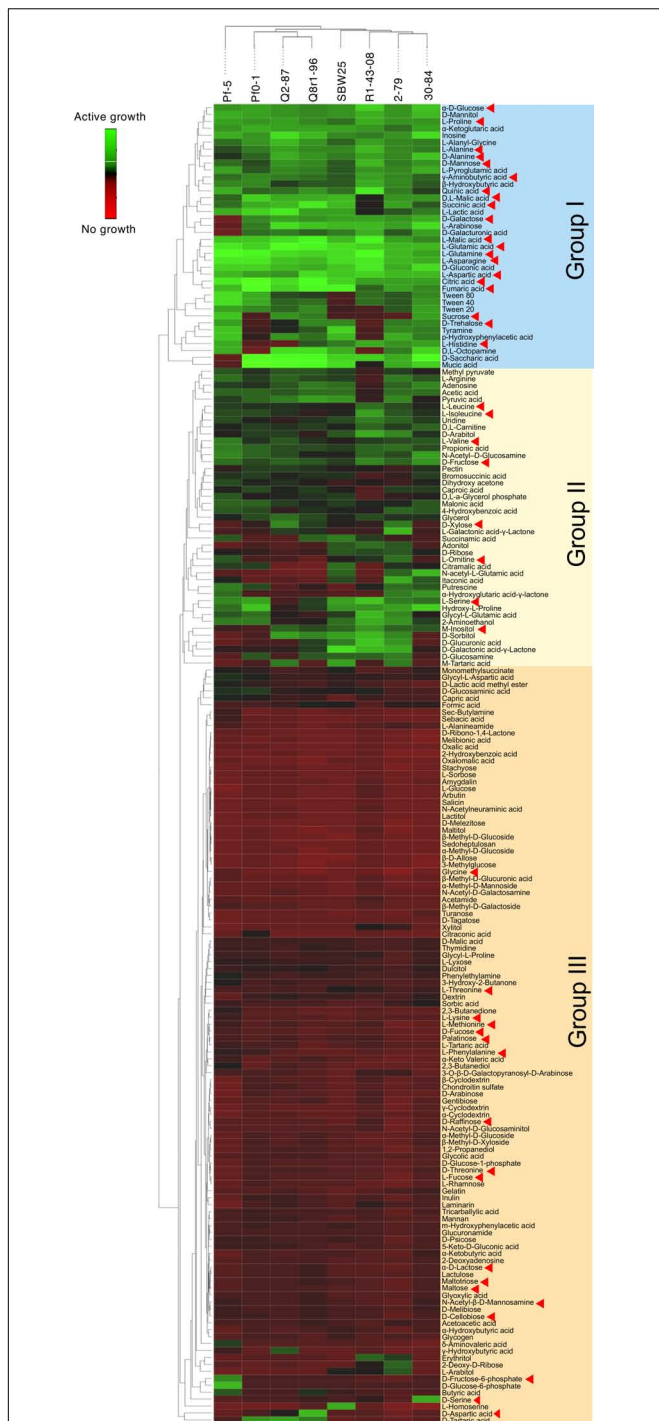


FIGURE 3 | Biolog Phenotype MicroArray profiling the eight rhizosphere *Pseudomonas* strains used in the study. The hierarchical clustering analysis was carried out using the average linkage method with Euclidean distances. Carbon sources identified by red arrowheads were also detected in the sterile root exudates of *B. distachyon* Bd21.

Although none of these differentially regulated pathways were shared by all eight strains, the cross-strain comparisons revealed several types of common and specific transcriptomic responses

that were elicited by the presence of plant exometabolites (Table 2). The visual representation of core gene expression patterns is provided in Supplementary Figure 5, which shows heatmaps of expression profiles and *p*-adj values for core genes shared by the studied strains. The figure is accompanied by Supplementary Table 13 that lists predicted functions of genes constituting the four distinct clusters observed after hierarchical clustering of gene expression values. The first category of shared differentially expressed pathways functioned in the uptake and catabolism of selected carbohydrates, quaternary ammonium compounds (QAs), and phenolics. All strains except for R1-43-08, responded to root exudates by inducing the fructose-specific phosphoenolpyruvate (PEP)-dependent phosphotransferase system (PTS^{Fru}). The components of this system are encoded by a conserved operon and include the cytoplasmic polyprotein EI/HPr/EIIA^{Fru} (FruB), the 1-phosphofructokinase FruK, and the fructose-specific permease EIIBC (FruA) (Chavarria et al., 2016). The PTS^{Fru} system functions by acquiring high-energy phosphates from PEP and sequentially passing them, *via* the EI/HPr/EIIA^{Fru} domains of FruB, to the EIIB component of FruA. The phosphates are ultimately transferred by the EIIC transporter to fructose yielding fructose 1-phosphate, which is channeled into the central metabolic pathways through the action of the phosphofructokinase FruK.

In all strains except for Q8r1-96 and Pf-5, the exposure to root exudates resulted in the induction of two genes adjacent to the *fru* cluster that encoded a Major Facilitator Superfamily (MFS) transporter and an L-arabinonate dehydratase (Table 2). These genes are predicted to participate in the uptake and catabolism of L-arabinose, where L-arabinonate dehydratase plays an important role by converting L-arabinonate to 2-dehydro-3-deoxy-L-arabinonate (Rahman et al., 2017). In SBW25, R1-43-08, and Q2-87, we also observed the induction of genes encoding components of the AraFGH complex, an ATP-Binding Cassette (ABC) superfamily transporter involved in the import of arabinose into the cell (Supplementary Tables 6, 7, 9). Finally, all strains except SBW25 and R1-43-08 responded to the presence of exudates by upregulating a conserved gene encoding an aldose epimerase superfamily protein. Such enzymes equilibrate alpha- and beta-anomers of aldoses and ensure that stereospecific enzymes involved in the metabolism of free sugars do not act as metabolic bottlenecks (Abayakoon et al., 2018). Although some aldose epimerases have been linked to specific pathways, the *Pseudomonas* gene identified in this study could not be assigned to a particular metabolic process based on sequence analysis and genomic location.

Several *Pseudomonas* strains responded to the presence of root exudates by upregulating genes involved in the uptake and catabolism of *myo*-inositol and possibly other stereoisomers of inositol (Table 2). The upregulated catabolic genes encode the dehydrogenase IolG, which oxidizes *myo*-inositol to its corresponding ketone, as well as IolE, IolD, IolB, and IolC that collectively convert the 2-keto-*myo*-inositol to acetyl-CoA and the glycolysis intermediate dihydroxyacetone phosphate (Yoshida et al., 2008; Kohler et al., 2011). In R1-43-08, Q8r1-96, Q2-87, and Pf-5, the upregulated functions

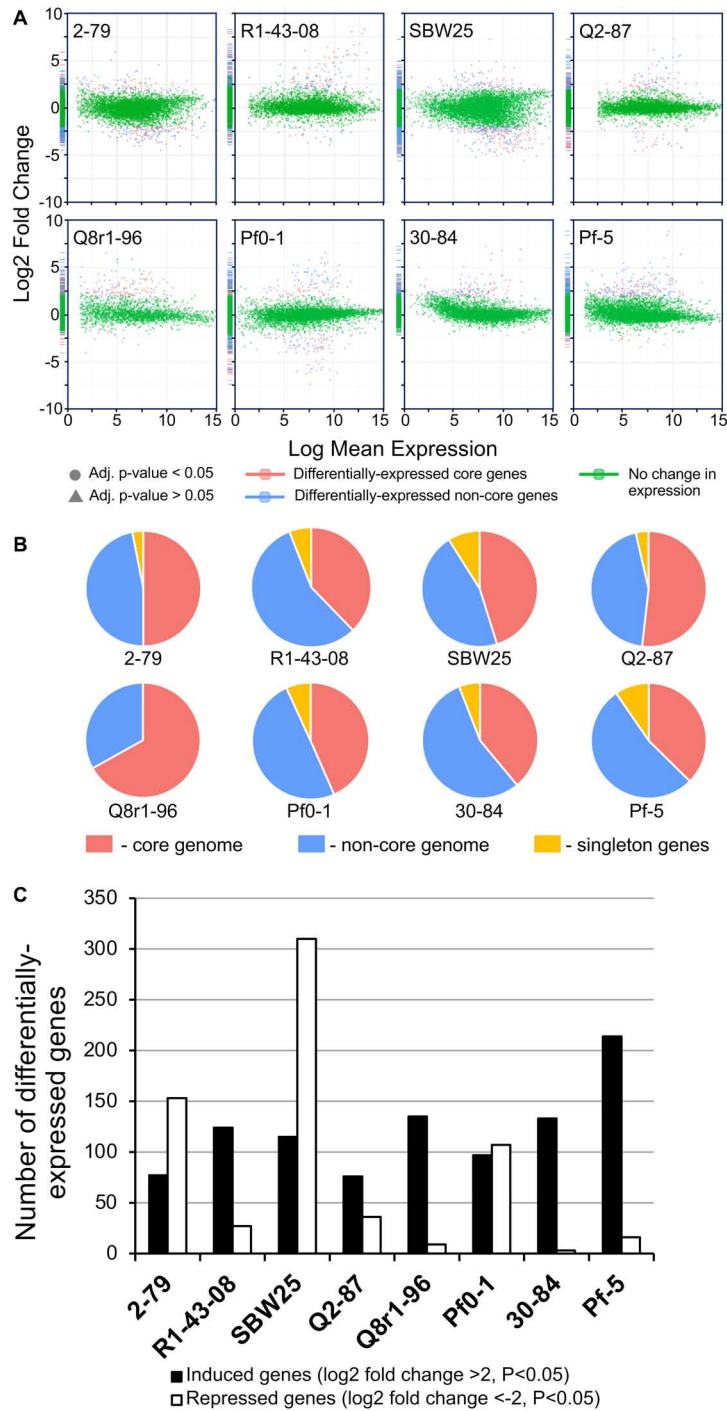


FIGURE 4 | (A) Log ratio versus abundance plots (MA-plots) showing the changes in gene expression in response to root exudates. The differentially expressed core and non-core genes are shown in red and blue, respectively. Green color indicates genes with a log₂ fold-change and/or adjusted *p* values below the established threshold. **(B)** Circular diagrams depicting the distribution of differentially expressed genes among the core, non-core, and singleton proteomes of individual *Pseudomonas* strains. **(C)** The number of genes per genome that were induced and repressed by *B. distachyon* root exudates.

also involved components of the putative inositol-specific ABC transporter. The cross-genome comparisons revealed that in all studied strains except for Pf0-1, components of the *myo*-inositol utilization pathway were encoded within a well-conserved gene cluster which, in addition to

catabolic and transport functions, also encodes a dedicated transcriptional repressor.

All studied strains of *Pseudomonas* carry multiple genes involved in scavenging the quaternary ammonium compounds choline, glycine betaine (GB), carnitine, choline-*O*-sulfate, and

TABLE 1 | The number of differentially expressed genes shared among the eight studied strains of rhizosphere *Pseudomonas*.

Strain	2-79	SBW25	R1-43-08	Q8r1-96	Q2-87	30-84	Pf0-1	Pf-5
2-79	260							
SBW25	101	425						
R1-43-08	30	25	151					
Q8r1-96	32	39	21	145				
Q2-87	27	28	25	31	112			
30-84	27	23	24	32	28	136		
Pf0-1	38	50	29	29	50	56	205	
Pf-5	36	41	52	86	29	55	40	230

The pairwise comparisons were conducted by BLASTp with the following cutoff parameters: E -value $\leq 1e-06$, minimum percent identity $\geq 40\%$, and minimum percent coverage $\geq 65\%$. The black diagonal cells show the number of differentially expressed genes per strain. In other words, these are self comparison values.

sarcosine from the environment. Many of these genes were differentially expressed, including those encoding parts of the ABC transporter CbcXWV, which is predicted to function in the uptake of choline under water-replete conditions (Table 2). Among enzymes induced in the presence of root exudates were the choline dehydrogenase BetA, which converts choline to glycine betaine and a network of enzymes (i.e., the Rieske family oxygenase GbcAB, the dimethylglycine demethylase DgcAB, and the sarcosine oxidase SoxBDAG) that sequentially convert GB to glycine. In 2-79 and SBW25, this group of differentially regulated genes also included an AraC-family transcriptional activator GbdR, which perceives intercellular levels of GB and induces genes involved in the transport and catabolism of glycine betaine and detoxification of the catabolic byproducts (Hampel et al., 2014).

The last category of activated catabolic pathways included the catechol branch of the β -ketoacid pathway for the degradation of aromatic compounds. In strains 30-84, Pf0-1, and Pf-5, growth on root exudates resulted in upregulation of catechol-1,2-dioxygenase, muconate cycloisomerase, and muconolactone isomerase, which collectively cleave the catechol ring and convert it to β -ketoacid enol-lactone (Harwood and Parales, 1996). Finally, analysis of the *P. synxantha* 2-79 transcriptome identified an induction of *benABC* genes encoding subunits of benzoate 1,2-dioxygenase, an oxidoreductase that generates catechol from benzoate.

In addition to various catabolic pathways, the exposure to root exudates also induced several genes involved in the homeostasis of copper (Table 2). Four of these genes form a conserved cluster in genomes of the strains and encode the periplasmic copper-sensing two-component system CinRS, the plastocyanin/azurin-like protein CinA, and the NADPH-dependent pre-Q₀ reductase CinQ. Also, in strains Q2-87, 30-84, Pf0-1, and Pf-5, we observed upregulation of a conserved operon encoding the multicopper oxidase CopA, the periplasmic copper-binding protein CopC, the inner membrane protein CopD, and outer membrane protein CopB. In several Gram-negative bacteria, these Cop proteins are thought to have dual functions and participate both in the uptake of essential copper as well as in the sequestration of excess copper in the periplasm and outer membrane.

The analysis of shared downregulated pathways revealed that most of the strains respond to the presence of root exudates by repressing genes involved in the uptake and catabolism of sulfur compounds (Table 2). In strains SBW25, R1-43-08, Q8r1-96, Q2-87, Pf0-1, and Pf-5, this response involved the *ssuEADCB* operon responsible for the utilization of alkanesulfonates as sulfur sources. The *ssu* operon is highly conserved in fluorescent pseudomonads and encodes the FMN₂-dependent monooxygenase SsuD and the NAD (P)H-dependent FMN reductase SsuE, which together catalyze the desulfonation of alkanesulfonates. Also, the *ssu* locus contains genes for the molybdopterin-binding protein SsuF and the alkanesulfonate-specific ABC-type transporter consisting of the sulfonate substrate-binding protein SsuA, sulfonate permease protein SsuC, and sulfonate transport ATP-binding protein SsuB. Finally, in R1-43-08, Q2-87, Pf0-1, and Pf-5, growth on root exudates coincided with repression of the *tauABCD* operon, which allows these strains to utilize taurine (2-aminoethanesulfonate) as a sulfur source. The repressed *tau* genes encoded the 2-oxoglutarate-dependent taurine dioxygenase TauD and substrate-binding, ATP-binding, and permease components of the taurine-specific ABC transporter TauABC.

Other Differentially Expressed Pathways

In addition to their effect on several shared cellular pathways, growth on root exudates resulted in the induction or repression of numerous strain-specific genes. In closely related *P. synxantha* 2-79 and *P. fluorescens* SBW25, we observed differential expression of genes involved in energy metabolism, transport of amino acids, and surface attachment (Supplementary Tables 5, 6). Other notable differentially expressed pathways included 2-79 gene clusters that encode enzymes for the catabolism of trehalose, a prophage, and toxin/antitoxin system, as well as the SBW25 operon predicted to control the synthesis of the capsular exopolysaccharide colonic acid. The response of *Pseudomonas* sp. R1-43-08 to root exudates also involved differential expression of different energy metabolism pathways. In addition, we observed the upregulation of genes involved in the uptake and catabolism of xylose (also upregulated in 2-79) and repression of enzymes for the biosynthesis of phenazine-1-carboxylic acid and assimilation of inorganic sulfur and L-cysteine biosynthesis (Supplementary Table 7).

The analysis of the Q8r1-96 transcriptome revealed perturbation of different metabolic pathways including genes encoding components of cytochrome C oxidase, transport and catabolism of sorbitol/mannitol, metabolism of butanoic acid, and biosynthesis of exopolysaccharides alginate and poly- β -1-6-*N*-acetylglucosamine (Supplementary Table 8). In *P. fluorescens* Q2-87, we identified differential expression of genes involved in metabolism of galactose, tryptophan, tyrosine, glycine, serine, and threonine (Supplementary Table 9), while in *P. chlororaphis* 30-84, growth on exudates activated the biosynthesis of molybdopterin cofactor, catabolism of galactonate and acetoin, and uptake and catabolism of putrescine (Supplementary Table 10). The response of *P. protegens* Pf-5 to root exudates involved upregulation of acetoin dehydrogenase, which converts acetoin to acetaldehyde and acetyl-CoA, as

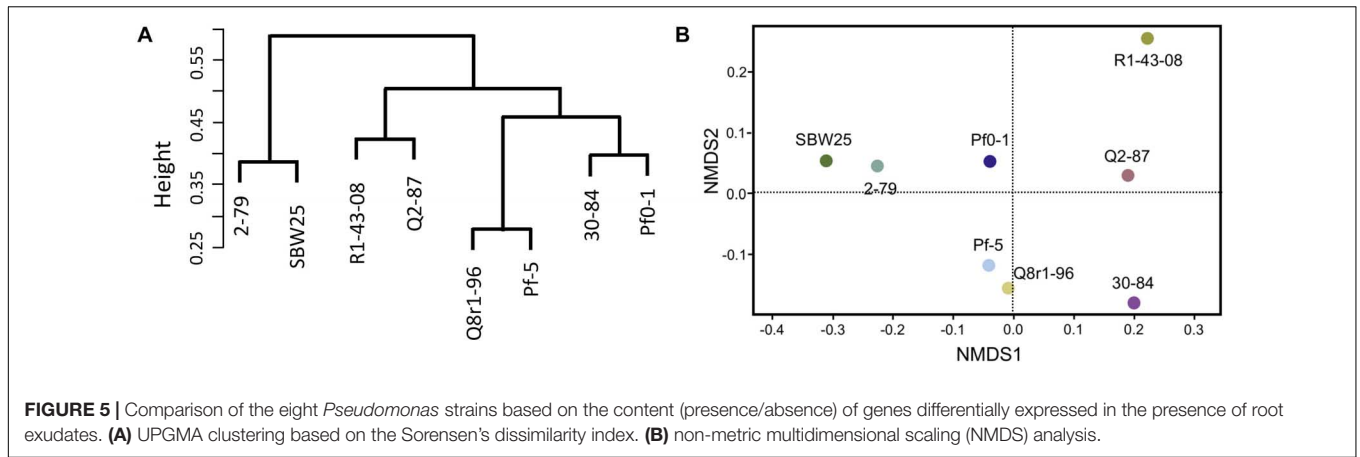


FIGURE 5 | Comparison of the eight *Pseudomonas* strains based on the content (presence/absence) of genes differentially expressed in the presence of root exudates. **(A)** UPGMA clustering based on the Sorensen's dissimilarity index. **(B)** non-metric multidimensional scaling (NMDS) analysis.

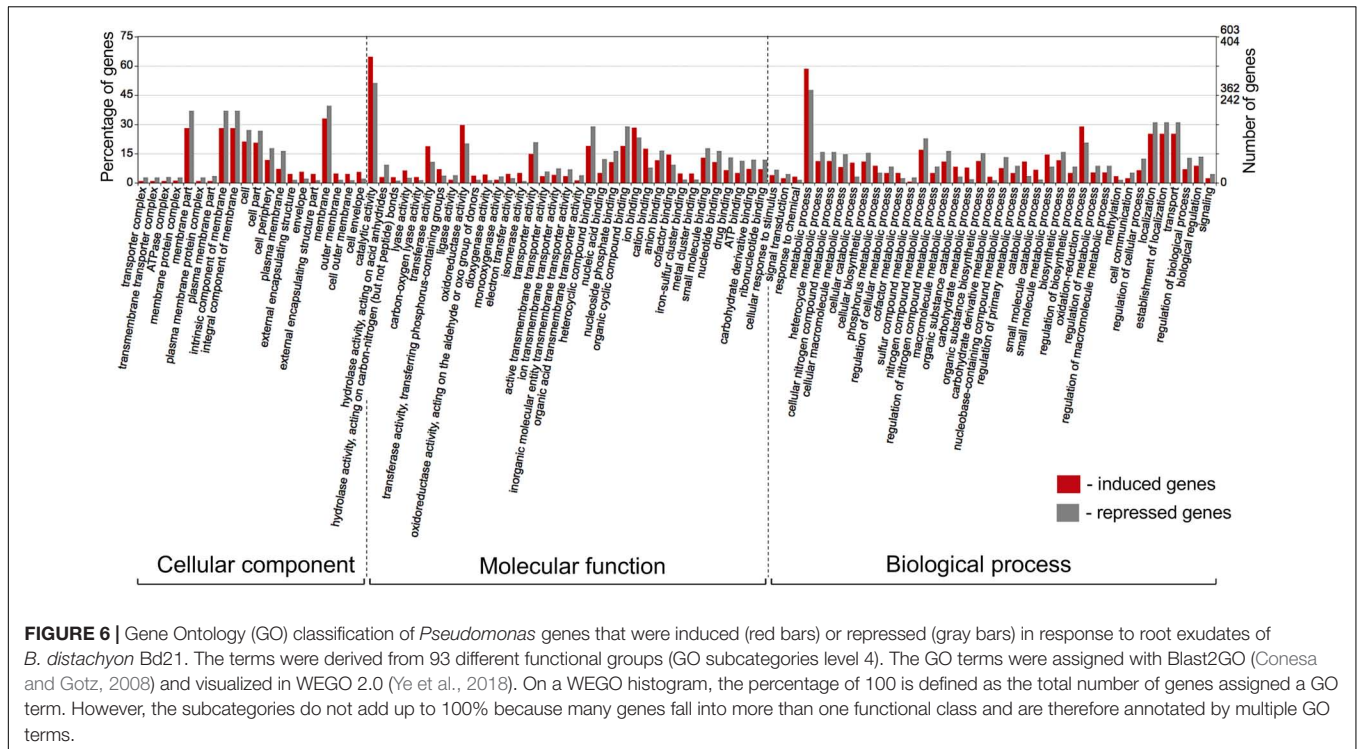


FIGURE 6 | Gene Ontology (GO) classification of *Pseudomonas* genes that were induced (red bars) or repressed (gray bars) in response to root exudates of *B. distachyon* Bd21. The terms were derived from 93 different functional groups (GO subcategories level 4). The GO terms were assigned with Blast2GO (Conesa and Gotz, 2008) and visualized in WEGO 2.0 (Ye et al., 2018). On a WEGO histogram, the percentage of 100 is defined as the total number of genes assigned a GO term. However, the subcategories do not add up to 100% because many genes fall into more than one functional class and are therefore annotated by multiple GO terms.

well as pathways for the utilization of glycolate and putrescine (Supplementary Table 11). Also induced were genes for the production of pyrrolnitrin and PhIG hydrolase, which modulate the metabolic loads attributed to the synthesis of 2,4-diacetylphloroglucinol. The differentially expressed genes of *P. fluorescens* Pf0-1 included, among others, operons encoding cytochrome C oxidase and enzymes for catabolism of malonic acid (Supplementary Table 12). Yet another interesting finding involved the induction of assorted genes acting in the homeostasis of iron and defense against reactive oxygen species (ROS). We observed activation of iron dicitrate transporters (SBW25 and 30-84), genes for the biosynthesis of siderophores ornicrogatin (SBW25) and pyochelin (Pf-5), heme-degrading enzymes (2-79, 30-84), TonB siderophore receptors, and components of the energy-transducing inner membrane

complex TonB-ExbB-ExbD (2-79 and Pf-5). The differentially expressed ROS defense pathways were represented by different catalases in strains 2-79, R1-43-08, Q8r1-96, Q2-87, Pf0-1, and Pf-5 and organic hydroperoxide resistance proteins in strains SBW25 and R1-43-08. Finally, in SBW25, Q2-87, 30-84, and Pf0-1, the addition of exudates resulted in the upregulation of peroxiredoxins that detoxify H₂O₂, peroxyxynitrite, and aliphatic and aromatic hydroperoxides.

DISCUSSION

Our analysis of *B. distachyon* root exudates revealed a complex mix of primary and secondary metabolites, thus supporting the view of the plant rhizosphere as a carbon-rich niche for

TABLE 2 | The distribution and predicted functions of selected differentially expressed genes^a.

Predicted function	Strain ^b							
	2-79	SBW25	R1-43-08	Q8r1-96	Q2-87	30-84	Pf0-1	Pf-5
Uptake and catabolism of fructose								
D-fructose PTS system, IIC component	2756598827 (2.7)	649634314 (2.3)		2597873629 (3.6)	2597850083 (2.7)	2597856046 (3.6)	637740645 (2.9)	637318202 (2.8)
1-phosphofructokinase	2756598828 (2.9)	649634313 (3.1)		2597873628 (3.9)	2597850082 (2.7)	2597856045 (3.4)	637740644 (3.1)	637318201 (2.7)
D-fructose PTS system, IIA component	2756598829 (2.6)	649634312 (3.0)		2597873627 (3.7)	2597850081 (2.6)	2597856044 (3.6)	637740643 (2.9)	637318200 (3.2)
Uptake and catabolism of arabinose								
MFS superfamily transporter	2756599521 (2.2)	649635836 (3.6)	2756590067 (4.9)		2597851595 (3.1)	2597859759 (4.2)	637743102 (2.9)	
L-arabinonate dehydratase	2756599520 (3.1)	649635835 (4.3)	2756590066 (5.5)		2597851594 (5.4)	2597859760 (4.0)	637743103 (3.5)	
Interconversion of alpha- and beta-anomers of aldoses								
Aldose epimerase superfamily protein	2756599919 (2.7)			2597878613 (4.2)	2597849545 (3.1)	2597860977 (4.2)	637742166 (3.4)	637323358 (3.5)
Uptake and catabolism of quaternary ammonium compounds								
Choline dehydrogenase BetA				2597874908 (2.3)	2597851450 (2.1)			
Transcriptional regulator GbdR	2756597125 (-3.7)	649639087 (-3.9)						
Membrane dipeptidase, <i>dgc</i> operon	2756597136 (1.9)		2756592046 (2.0)	2597878321 (3.8)	2597849833 (2.9)	2597860696 (2.6)		637323077 (3.3)
Hypothetical protein, <i>dgcAB</i> operon	2756597137 (2.4)		2756592045 (2.3)	2597878320 (3.4)	2597849834 (2.7)	2597860695 (2.3)		637323076 (3.3)
Dimethyl Gly demethylase DgcA	2756597138 (2.7)		2756592044 (2.0)	2597878317 (3.3)	2597849835 (2.7)	2597860694 (2.2)		637323075 (3.2)
Dimethyl Gly demethylase DgcB	2756597139 (2.3)			2597878318 (3.6)	2597849836 (2.6)	2597860693 (2.4)		637323074 (3.0)
Betaine demethylase, GbcA subunit	2756597143 (2.1)		2756592039 (2.3)	2597878312 (4.3)				637323070 (3.7)
Betaine demethylase, GbcB subunit				2597878311 (3.9)		2597860689 (2.0)		637323069 (3.2)
Ser hydroxymethyltransferase, <i>sox</i> operon	2756597149 (2.1)		2756592033 (2.0)	2597878308 (2.9)	2597849846 (2.7)			637323064 (3.1)
Sarcosine oxidase, γ subunit, SoxG				2597878304 (2.9)				
Sarcosine oxidase, α subunit, SoxA			2756592028 (2.1)	2597878305 (3.0)				637323061 (2.4)
Sarcosine oxidase, δ subunit, SoxD				2597878306 (2.5)				637323062 (2.2)
Sarcosine oxidase, β subunit, SoxB	2756597150 (2.4)		2756592032 (1.9)	2597878307 (2.6)				637323063 (2.3)
Betaine substrate-binding protein CbcX			2756590368 (2.3)	2597878336 (2.3)	2597850794 (3.1)		637742655 (-3.5)	
ABC transporter, ATP-binding protein CbcV				2597878338 (2.3)			637742656 (-3.5)	
Uptake and catabolism of myo-inositol								
5-dehydro-2-deoxygluconokinase, lolC			2756592881 (2.5)	2597876275 (4.3)		2597857598 (2.4)		637319925 (4.2)
2-keto-myo-inositol dehydratase, lolE			2756592884 (2.5)	2597876273 (4.6)		2597857602 (2.4)		637319928 (4.1)
5-deoxy-glucuronate isomerase, lolB			2756592883 (2.3)	2597876272 (4.3)		2597857600 (2.4)		637319927 (4.3)
2-keto-myo-inositol isomerase, lolL			2756592882 (2.7)			2597857599 (2.4)		637319926 (4.4)
3D-(3,5/4)-trihydroxycyclohexane-1,2-dione acylhydrolase, lolD			2756592885 (2.4)	2597876269 (4.8)		2597857603 (2.5)		637319929 (4.3)
Myo-inositol 2-dehydrogenase, lolG	2756595203 (1.9)		2756592886 (2.2)	2597876268 (4.8)		2597857604 (2.0)		637319930 (3.9)
Inositol transport substrate-binding protein			2756592888 (2.0)	2597876265 (3.8)	2597851513 (2.8)			637319932 (3.8)
Inositol transport permease protein			2756592890 (1.9)	2597876263 (3.6)	2597851515 (2.2)			637319934 (3.5)
Inositol transport ATP-binding protein			2756592889 (2.2)	2597876264 (3.8)	2597851514 (2.7)			637319933 (3.6)

(Continued)

TABLE 2 | Continued

Predicted function	Strain ^b							
	2-79	SBW25	R1-43-08	Q8r1-96	Q2-87	30-84	Pf0-1	Pf-5
Uptake and catabolism of fructose								
Catabolism of phenolics								
Muconate cycloisomerase						2597859089 (3.1)	637742838 (3.4)	637321199 (4.8)
Muconolactone delta-isomerase						2597859088 (2.6)	637742837 (3.5)	637321198 (4.4)
Catechol 1,2-dioxygenase						2597859087 (2.0)	637742836 (2.9)	637321197 (3.5)
AraC-type DNA-binding protein						2597859086 (2.0)		637321196 (2.2)
Benzoate 1,2-dioxygenase, α subunit	2756599329 (2.7)					2597859085 (3.4)	637742843 (3.9)	637321195 (3.8)
Benzoate 1,2-dioxygenase, β subunit	2756599330 (2.2)					2597859084 (3.3)	637742842 (4.2)	637321194 (4.8)
Benzoate 1,2-dioxygenase, reductase subunit	2756599331 (2.1)					2597859083 (3.4)	637742841 (3.9)	637321193 (4.3)
Copper homeostasis								
pre-Q ₀ reductase/7-cyano-7-deazaguanine reductase CinQ	2756597439 (2.7)	649635068 (1.8)		2597874689 (3.4)				637319306 (2.5)
Cupredoxin-like copper-binding protein CinA	2756597440 (2.8)	649635067 (4.3)	2756590986 (2.03)		2597853017 (7.3)	2597857153 (5.7)	637743734 (3.5)	637319305 (3.4)
Heavy metal response regulator CinR		649635066 (1.8)		2597874687 (2.1)	2597853018 (3.2)	2597857152 (2.4)	637743735 (2.1)	637319304 (2.5)
Heavy metal sensor histidine kinase CinS		649635065 (2.0)				2597857151 (2.2)	637743736 (2.0)	637319303 (2.0)
Copper resistance protein CopA				2597877412 (5.9)	2597850492 (5.6)	2597857966 (6.9)	637743691 (5.2)	637320232 (6.4)
Copper resistance protein CopB					2597850491 (5.3)	2597857965 (6.8)	637743692 (5.5)	637320231 (6.0)
Copper resistance protein CopC					2597850490 (4.6)	2597857964 (7.2)	637743693 (5.4)	
Copper resistance protein CopD					2597850489 (4.9)	2597857963 (6.9)	637743694 (5.2)	
Conserved hypothetical protein								
Aldose epimerase superfamily protein	2756599919 (2.7)			2597878613 (4.2)	2597849545 (3.1)	2597860977 (4.2)	637742166 (3.4)	637323358 (3.5)
Uptake and catabolism of sulfonates								
FMN-dependent monooxygenase SsuE			2756592254 (-1.9)				637745334 (-3.5)	
Sulfonate substrate-binding protein SsuA		649639261 (-2.0)	2756592253 (-2.2)	2597878518 (-2.6)	2597849636 (-3.9)		637745333 (-7.0)	637323272 (-2.7)
FMN-dependent monooxygenase SsuD		649639260 (-1.9)	2756592252 (-2.3)		2597849637 (-2.8)		637745332 (-5.8)	637323271 (-2.3)
Sulfonate permease protein SsuC		649639259 (-2.4)	2756592251 (-2.1)	2597878516 (-1.9)	2597849638 (-3.2)		637745331 (-5.8)	637323270 (-2.5)
Sulfonate transport ATP-binding protein SsuB		649639258 (-2.5)	2756592250 (-2.3)		2597849639 (-2.5)		637745330 (-5.6)	637323269 (-2.7)
Molybdopterin binding protein SsuF		649639257 (-3.1)	2756592249 (-2.7)	2597878514 (-2.9)	2597849641 (-3.3)		637745339 (-6.2)	637323268 (-2.7)
Uptake and catabolism of taurine								
Taurine substrate-binding protein TauA					2597854917 (-2.0)		637740095 (-4.1)	
Taurine transport ATP-binding protein TauB			2756592398 (-1.9)				637740094 (-3.7)	637317614 (-1.9)
Taurine permease protein TauC			2756592398 (-1.9)				637740093 (-3.9)	637317613 (-2.0)
Taurine dioxygenase TauD					2597854920 (-1.8)		637740092 (-3.6)	

^aThe shared differentially expressed genes were identified by BLASTp with the cutoff parameters of E-value $\leq 1e-06$, minimum percent identity $\geq 40\%$, and minimum percent coverage $\geq 65\%$.

^bValues in columns indicate JGI IMG gene IDs followed by the corresponding fold-change (FC) values (shown in brackets).

soil microorganisms. Our results were in agreement with a recent report of 27 different sugars, amino acids, and organic acids in *Brachypodium* exudates (Kawasaki et al., 2016). We confirmed the presence of exometabolites identified in that study, along with dozens of additional analytes that were identified by matching their mass-spectra and retention indices to the LECO/Fiehn Metabolomics library (**Supplementary Table 3**). The complementation of the metabolomic analysis with profiling of the bacteria by Biolog Phenotype MicroArrays revealed that a substantial proportion of the characterized exudate constituents were catabolized by a collection of eight *Pseudomonas* strains from across the *P. fluorescens* group that is known to form associations with plant roots. The amendment of *Pseudomonas* cultures with root exudates caused changes in the expression of multiple genes encoding catabolic and anabolic enzymes, predicted transporters, transcriptional regulators, stress response, and conserved hypothetical proteins. In most strains, these differentially expressed genes were almost equally split between the core and variable genome regions, mirroring the substantial strain-to-strain variation in the genome size and gene content within the *P. fluorescens* species complex (Loper et al., 2012).

The analysis of transcriptome responses to root exudates revealed several types of cellular pathways present in the strains used in this study. The first category of such pathways was involved in the catabolism of carbohydrates such as fructose, arabinose, *myo*-inositol, xylose, trehalose, and galactose. Among these catabolic traits, the ability to utilize fructose as a carbon source is highly conserved among fluorescent pseudomonads. In contrast, growth on arabinose, *myo*-inositol, xylose, and trehalose is variably present and was traditionally used to differentiate species and biovars within the *P. fluorescens* group (Barrett et al., 1986). We speculate that such variably distributed pathways contribute to the differential affinity of pseudomonads toward host plants and/or to determine which strains flourish in response to growing roots and changing environments. Several independent studies have confirmed the importance of carbohydrate catabolism pathways for the biology of rhizosphere pseudomonads. For example, *in vivo* expression technology (IVET) profiling of *P. fluorescens* SBW25 identified xylose isomerase among genome regions essential for the colonization of sugar beet seedlings (Liu et al., 2015), whereas a genome-wide Tn-Seq screen of *Pseudomonas simiae* identified genes for the catabolism of *myo*-inositol among traits essential for the colonization of *Arabidopsis thaliana* roots (Cole et al., 2017).

The response of rhizosphere *Pseudomonas* to *Brachypodium* root exudates also involved pathways for the uptake and metabolism of amino acids. We observed differential expression of genes encoding the hydrophobic (HAAT) and polar (PAAT) amino acid uptake transporters in strains 2-79, SBW25, Q2-87, Pf0-1, and Pf-5. Other related genes encoded enzymes for the catabolism of valine and glutamic acid (2-79); metabolism of tryptophan, glycine, serine, and threonine (Q2-87); and biosynthesis of methionine (Q8r1-96). It is plausible that the abundance of amino acids in root exudates is also linked to the repression of pathways

involved in the catabolism of sulfonates and taurine that was observed in several strains (**Table 2**). Although the preferred source of sulfur for *P. fluorescens* is unknown, in the closely related *P. aeruginosa*, the sulfur starvation response is triggered by the growth on any sulfur compound other than sulfate, thiocyanate, and cysteine (Hummerjohann et al., 1998). This fact, together with the presence of cysteine and cystine in the root exudates, suggest that root exudates of *Brachypodium* may serve as an important source of sulfur for rhizosphere *Pseudomonas*. These findings also agree well with the reported scarcity of inorganic sulfate in the soil, and the presence of sulfur mostly in the form of organic compounds, including amino acids, proteins, sulfate esters, and sulfonates (Autry and Fitzgerald, 1990).

Another interesting result of this study was the concerted activation of copper and iron homeostasis pathways observed in all of the *Pseudomonas* strains used in this work. In bacteria, an excess of copper is toxic and triggers oxidative stress due to the formation of free radicals, as well as disruption of protein metalation and stability of iron-sulfur clusters (Bondarczuk and Piotrowska-Seget, 2013). On the other hand, copper is an essential trace element used as a cofactor in different enzymes. Similarly, although elevated levels of iron cause redox stress, this element is also found in active energy metabolism enzymes and is crucial for bacterial growth (Andrews et al., 2003). The analysis of metal homeostasis genes identified in this study suggests that their induction was likely triggered by the deficiency of copper and iron in bacterial cultures grown in the presence of root exudates. We attribute this effect to the ability of some components of root exudates to chelate soil metals.

Despite the abundance of iron in the soil, its bioavailability is limited due to the low solubility of Fe (III) oxyhydrates at neutral pH. The non-graminaceous plants circumvent this problem by acidifying the rhizosphere and secreting flavins, phenolics, and organic acids that chelate iron. The reduction of these ferric chelates releases soluble ferrous iron taken up by root cells (Kobayashi and Nishizawa, 2012). Graminaceous plants, like *Brachypodium*, acquire iron by secreting into the soil non-protein amino acids of the mugineic acid (MA) group, which act as Fe (III)-chelating phytosiderophores. In addition to iron, low-molecular-weight organic acids and phytosiderophores bind other divalent and trivalent metals (including copper) and contribute to heavy-metal tolerance in plants (Chen et al., 2017). It is plausible that the presence of these plant exometabolites is responsible for the deficit of iron and copper observed in *Pseudomonas* cultures grown in the presence of root exudates. These results further underscore the importance of diverse and redundant metal homeostasis pathways found in genomes of the *P. fluorescens* group for the ability of these organisms to colonize and persist in the plant rhizosphere.

Recently, Klonowska et al. (2018) examined transcriptomic responses of symbiotic nitrogen-fixing bacteria to root exudates of the legume plant *Mimosa pudica*, which has an unusual ability to support both alpha- (*Rhizobium*) and beta-rhizobia (*Cupriavidus* and *Burkholderia*). Using RNA-seq, the authors characterized genes involved in the perception of root exudates in the nodulating bacteria *Burkholderia phymatum*

STM815, *Cupriavidus taiwanensis* LMG19424, and *Rhizobium mesoamericanum* STM3625. Interestingly, the analysis of differentially expressed genes revealed induction of pathways involved in the catabolism of fructose, xylose, *myo*-inositol, and protocatechuate/catechol. Also upregulated were some copper homeostasis, siderophore biosynthesis, and oxidative stress genes. Finally, the analytical profiling of *M. punica* exudates revealed an overlap with *Brachypodium* in the types of carbohydrates, amino acids, and organic acids present. These findings suggest that differentially expressed genes shared by multiple strains of the group *P. fluorescens* are not unique to the *Brachypodium*-*Pseudomonas* system but represent a set of conserved cellular pathways involved in the perception of plant exometabolites by different clades of rhizosphere-dwelling *Proteobacteria*.

Most strains included in this study were originally selected based on the ability to colonize the rhizosphere and produce secondary metabolites that alleviate the plant stress response and/or inhibit soilborne pathogens. It has been suggested that plant metabolites released into the rhizosphere affect the biocontrol activity of plant-beneficial pseudomonads (de Werra et al., 2011). We provide further support to this hypothesis by demonstrating that in some strains, root exudates modulate the expression of genes for the catabolism of the plant growth-promoting metabolites acetoin and 2,3-butanediol. The exposure to exudates also affected the expression of genes for the synthesis of well-characterized antifungal compounds pyrrolnitrin, phenazine-1-carboxylic acid, and 2,4-diacetylphloroglucinol. The modulatory effects were strain-specific, suggesting significant differences in the regulatory networks involved in the perception of plant signals and regulation of the production of antibiotics and growth-promoting metabolites.

The final significant finding of this study was the induction of catabolism of quaternary amines (QAs) observed in multiple strains of the *P. fluorescens* group during growth on root exudates. This observation was supported by the detection of glycine betaine in the root secretions of *B. distachyon*. The presence of QAs in plant tissues and the capacity of these metabolites to provide stress protection and nutrients to plant pathogens and symbionts were reported before (Boncompagni et al., 1999; Chen et al., 2013; Kabbadj et al., 2017), but our study is among the first to highlight the potential importance of these metabolites for rhizosphere interactions. Pseudomonads do not synthesize QAs *de novo* but have evolved many pathways to scavenge them from eukaryotic hosts, where these metabolites are abundant due to the prominence of phosphatidylcholine in cellular membranes. Strains of *P. fluorescens* carry genes for the conversion of choline, carnitine, and glycine betaine to glycine, as well as quaternary amine transporters of the BCCT and ABC families that are also conserved in the opportunistic human pathogen *P. aeruginosa* and the plant pathogen *P. syringae* (Galvao et al., 2006; Chen et al., 2013; Wargo, 2013b).

In *P. aeruginosa*, choline catabolism genes are essential for the ability of this pathogen to persist during lung infection (Wargo, 2013a). Similarly, a *P. syringae* mutant deficient in BetT, OpuC, and CbcXWV quaternary amine transporters had

reduced fitness during colonization of bean and soybean leaves under greenhouse and field conditions (Chen et al., 2013). Depending on water availability, *P. aeruginosa* and *P. syringae* catabolize exogenously supplied QAs as carbon and nitrogen sources or accumulate them as osmoprotectants (Chen et al., 2013; Wargo, 2013b). Our ongoing work in *P. synxantha* 2–79 unraveled similar physiological responses and demonstrated that QA transporters function differentially and redundantly in the uptake of quaternary amines as nutrients (Pablo and Mavrodi, unpublished). In contrast, under water stress, the QAs choline, betaine, and carnitine are accumulated preferentially for osmoprotection. Under drought stress, a 2–79 mutant devoid of all known QA transporters was less competitive in the colonization of the *Brachypodium* rhizosphere than its wild-type parental strain. Interestingly, our metabolomic profiling of root exudates also revealed proline, glutamine, and hydroxyectoine. These metabolites act as compatible solutes in different groups of microorganisms (Yancey et al., 1982; Empadinhas and da Costa, 2008), suggesting an important role of root exudates in the ability of *Pseudomonas* to persist in the rhizosphere of drought-stressed plants.

DATA AVAILABILITY STATEMENT

The original contributions presented in the study are publicly available. This data can be found here: NCBI BioProject accession numbers PRJNA439743 through PRJNA439790.

AUTHOR CONTRIBUTIONS

DM, OM, and LT conceived the research project. OM and JM collected root exudates. OM and DM cultured strains and extracted total RNA. AB and DG performed metabolomic analysis of root exudates. DM, JP, and AF analyzed RNA-seq data. LE, KH, and IP conducted Biolog analyses. DM, AF, OM, DW, and LT wrote the manuscript. All authors contributed to the manuscript revision.

FUNDING

This study was funded by NSF grant IOS-1656872 and by an award from the DOE Joint Genome Institute's Community Science Program. The authors also acknowledge support from Australian Research Council Discovery grant (DP160103746) and Mississippi INBRE, funded by an Institutional Development Award (IDeA) from the National Institute of General Medical Sciences of the National Institutes of Health under grant P20GM103476.

SUPPLEMENTARY MATERIAL

The Supplementary Material for this article can be found online at: <https://www.frontiersin.org/articles/10.3389/fmicb.2021.651282/full#supplementary-material>

REFERENCES

- Abayakoon, P., Lingford, J. P., Jin, Y., Bengt, C., Davies, G. J., Yao, S., et al. (2018). Discovery and characterization of a sulfoquinovose mutarotase using kinetic analysis at equilibrium by exchange spectroscopy. *Biochem. J.* 475, 1371–1383. doi: 10.1042/bcj20170947
- Andrews, S. C., Robinson, A. K., and Rodriguez-Quinones, F. (2003). Bacterial iron homeostasis. *FEMS Microbiol. Rev.* 27, 215–237. doi: 10.1016/s0168-6445(03)00055-x
- Arkin, A. P., Cottingham, R. W., Henry, C. S., Harris, N. L., Stevens, R. L., Maslov, S., et al. (2018). KBase: the United States department of energy systems biology knowledgebase. *Nat. Biotechnol.* 36, 566–569.
- Autry, A. R., and Fitzgerald, J. W. (1990). Sulfonate S: a major form of forest soil organic sulfur. *Biol. Fertil. Soils* 10, 50–56.
- Babicki, S., Arndt, D., Marcu, A., Liang, Y., Grant, J. R., Maciejewski, A., et al. (2016). Heatmapper: web-enabled heat mapping for all. *Nucleic Acids Res.* 44, W147–W153.
- Badri, D. V., and Vivanco, J. M. (2009). Regulation and function of root exudates. *Plant Cell Environ.* 32, 666–681. doi: 10.1111/j.1365-3040.2009.01926.x
- Badri, D. V., Weir, T. L., Van Der Lelie, D., and Vivanco, J. M. (2009). Rhizosphere chemical dialogues: plant-microbe interactions. *Curr. Opin. Biotechnol.* 20, 642–650. doi: 10.1016/j.copbio.2009.09.014
- Bais, H. P., Prithiviraj, B., Jha, A. K., Ausubel, F. M., and Vivanco, J. M. (2005). Mediation of pathogen resistance by exudation of antimicrobials from roots. *Nature* 434, 217–221. doi: 10.1038/nature03356
- Bais, H. P., Weir, T. L., Perry, L. G., Gilroy, S., and Vivanco, J. M. (2006). The role of root exudates in rhizosphere interactions with plants and other organisms. *Annu. Rev. Plant Biol.* 57, 233–266. doi: 10.1146/annurev.arplant.57.032905.105159
- Bangera, M. G., and Thomashow, L. S. (1996). Characterization of a genomic locus required for synthesis of the antibiotic 2,4-diacetylphloroglucinol by the biological control agent *Pseudomonas fluorescens* Q2-87. *Mol. Plant Microbe Interact.* 9, 83–90.
- Barret, M., Frey-Klett, P., Guillerme-Erckelboudt, A. Y., Boutin, M., Guernec, G., and Sarniguet, A. (2009). Effect of wheat roots infected with the pathogenic fungus *Gaeumannomyces graminis* var. *tritici* on gene expression of the biocontrol bacterium *Pseudomonas fluorescens* Pf29Arp. *Mol. Plant-Microbe Interact.* 22, 1611–1623. doi: 10.1094/mpmi-22-12-1611
- Barrett, E. L., Solanes, R. E., Tang, J. S., and Palleroni, N. J. (1986). *Pseudomonas fluorescens* biovar V: its resolution into distinct component groups and the relationship of these groups to other *P. fluorescens* biovars, to *P. putida*, and to psychrotrophic pseudomonads associated with food spoilage. *J. Gen. Microbiol.* 132, 2709–2721. doi: 10.1099/00221287-132-10-2709
- Bevan, M. W., Garvin, D. F., and Vogel, J. P. (2010). *Brachypodium distachyon* genomics for sustainable food and fuel production. *Curr. Opin. Biotechnol.* 21, 211–217. doi: 10.1016/j.copbio.2010.03.006
- Boncompagni, E., Osteras, M., Poggi, M. C., and Le Rudulier, D. (1999). Occurrence of choline and glycine betaine uptake and metabolism in the family *Rhizobiaceae* and their roles in osmoprotection. *Appl. Environ. Microbiol.* 65, 2072–2077. doi: 10.1128/aem.65.5.2072-2077.1999
- Bondarczuk, K., and Piotrowska-Seget, Z. (2013). Molecular basis of active copper resistance mechanisms in Gram-negative bacteria. *Cell Biol. Toxicol.* 29, 397–405. doi: 10.1007/s10565-013-9262-1
- Brkljacic, J., Grotewold, E., Scholl, R., Mockler, T., Garvin, D. F., Vain, P., et al. (2011). *Brachypodium* as a model for the grasses: today and the future. *Plant Physiol.* 157, 3–13.
- Camacho-Carvajal, M. M. (2001). *Molecular Characterization of the Roles of Type 4 pili, NDH-I and PyrR in Rhizosphere Colonization of Pseudomonas fluorescens* WCS365. Dissertation, University of Leiden, Leiden.
- Chavarría, M., Goni-Moreno, A., De Lorenzo, V., and Nikel, P. I. (2016). A metabolic widget adjusts the phosphoenolpyruvate-dependent fructose influx in *Pseudomonas putida*. *mSystems* 1:e00154-16.
- Chen, C., Li, S., McKeever, D. R., and Beattie, G. A. (2013). The widespread plant-colonizing bacterial species *Pseudomonas syringae* detects and exploits an extracellular pool of choline in hosts. *Plant J.* 75, 891–902. doi: 10.1111/tjp.12262
- Chen, X., Zhang, Y., Zhang, Z., Zhao, Y., Sun, C., Yang, M., et al. (2018). PGAweb: a web server for bacterial pan-genome analysis. *Front. Microbiol.* 9:1910. doi: 10.3389/fmicb.2018.01910
- Chen, Y. T., Wang, Y., and Yeh, K. C. (2017). Role of root exudates in metal acquisition and tolerance. *Curr. Opin. Plant Biol.* 39, 66–72. doi: 10.1016/j.pbi.2017.06.004
- Cole, B. J., Feltcher, M. E., Waters, R. J., Wetmore, K. M., Mucyn, T. S., Ryan, E. M., et al. (2017). Genome-wide identification of bacterial plant colonization genes. *PLoS Biol.* 15:e2002860. doi: 10.1371/journal.pbio.2002860
- Conesa, A., and Gotz, S. (2008). Blast2GO: a comprehensive suite for functional analysis in plant genomics. *Int. J. Plant Genomics* 2008:619832.
- Curl, E. A., and Truelove, B. (1986). *The Rhizosphere*. Berlin: Springer-Verlag.
- Darzi, Y., Letunic, I., Bork, P., and Yamada, T. (2018). iPath3.0: interactive pathways explorer v3. *Nucleic Acids Res.* 46, W510–W513.
- de Weert, S., Dekkers, L., Bitter, W., Tuinman, S., Wijffes, A., Van Boxtel, R., et al. (2006). The two-component *colR/S* system of *Pseudomonas fluorescens* WCS365 plays a role in rhizosphere competence through maintaining the structure and function of the outer membrane. *FEMS Microbiol. Ecol.* 58, 205–213. doi: 10.1111/j.1574-6941.2006.00158.x
- de Weert, S., Vermeiren, H., Mulders, I. H., Kuiper, I., Hendrickx, N., Bloemberg, G. V., et al. (2002). Flagella-driven chemotaxis towards exudate components is an important trait for tomato root colonization by *Pseudomonas fluorescens*. *Mol. Plant Microbe Interact.* 15, 1173–1180. doi: 10.1094/mpmi.2002.15.11.1173
- de Werra, P., Huser, A., Tabacchi, R., Keel, C., and Maurhofer, M. (2011). Plant- and microbe-derived compounds affect the expression of genes encoding antifungal compounds in a pseudomonad with biocontrol activity. *Appl. Environ. Microbiol.* 77, 2807–2812. doi: 10.1128/aem.01760-10
- Dekkers, L. C., Phoelich, C. C., Van Der Fits, L., and Lugtenberg, B. J. (1998). A site-specific recombinase is required for competitive root colonization by *Pseudomonas fluorescens* WCS365. *Proc. Natl. Acad. Sci. U.S.A.* 95, 7051–7056. doi: 10.1073/pnas.95.12.7051
- De-la-Pena, C., Lei, Z., Watson, B. S., Sumner, L. W., and Vivanco, J. M. (2008). Root-microbe communication through protein secretion. *J. Biol. Chem.* 283, 25247–25255. doi: 10.1074/jbc.m801967200
- Empadinhas, N., and da Costa, M. S. (2008). Osmoadaptation mechanisms in prokaryotes: distribution of compatible solutes. *Int. Microbiol.* 11, 151–161.
- Espinosa-Urgel, M., Salido, A., and Ramos, J. L. (2000). Genetic analysis of functions involved in adhesion of *Pseudomonas putida* to seeds. *J. Bacteriol.* 182, 2363–2369. doi: 10.1128/jb.182.9.2363-2369.2000
- Fuqua, C. (2010). Passing the baton between laps: adhesion and cohesion in *Pseudomonas putida* biofilms. *Mol. Microbiol.* 77, 533–536. doi: 10.1111/j.1365-2958.2010.07250.x
- Galvao, T. C., De Lorenzo, V., and Canovas, D. (2006). Uncoupling of choline-O-sulphate utilization from osmoprotection in *Pseudomonas putida*. *Mol. Microbiol.* 62, 1643–1654. doi: 10.1111/j.1365-2958.2006.05488.x
- Garrido-Sanz, D., Meier-Kolthoff, J. P., Göker, M., Martín, M., Rivilla, R., and Redondo-Nieto, M. (2016). Genomic and genetic diversity within the *Pseudomonas fluorescens* complex. *PLoS One* 11:e0150183. doi: 10.1371/journal.pone.0150183
- Halverson, L. J., and Firestone, M. K. (2000). Differential effects of permeating and nonpermeating solutes on the fatty acid composition of *Pseudomonas putida*. *Appl. Environ. Microbiol.* 66, 2414–2421. doi: 10.1128/aem.66.6.2414-2421.2000
- Hampel, K. J., Labauve, A. E., Meadows, J. A., Fitzsimmons, L. F., Nock, A. M., and Wargo, M. J. (2014). Characterization of the GbdR regulon in *Pseudomonas aeruginosa*. *J. Bacteriol.* 196, 7–15. doi: 10.1128/jb.01055-13
- Harwood, C. S., and Parales, R. E. (1996). The beta-ketoadipate pathway and the biology of self-identity. *Annu. Rev. Microbiol.* 50, 553–590. doi: 10.1146/annurev.micro.50.1.553
- Hesse, C., Schulz, F., Bull, C. T., Shaffer, B. T., Yan, Q., Shapiro, N., et al. (2018). Genome-based evolutionary history of *Pseudomonas* spp. *Environ. Microbiol.* 20, 2142–2159.
- Hinsa, S. M., Espinosa-Urgel, M., Ramos, J. L., and O'Toole, G. A. (2003). Transition from reversible to irreversible attachment during biofilm formation by *Pseudomonas fluorescens* WCS365 requires an ABC transporter and a large secreted protein. *Mol. Microbiol.* 49, 905–918. doi: 10.1046/j.1365-2958.2003.03615.x
- Højberg, O., Schnider, U., Winteler, H. V., Sorensen, J., and Haas, D. (1999). Oxygen-sensing reporter strain of *Pseudomonas fluorescens* for monitoring

- the distribution of low-oxygen habitats in soil. *Appl. Environ. Microbiol.* 65, 4085–4093. doi: 10.1128/aem.65.9.4085-4093.1999
- Hong, S. Y., Park, J. H., Cho, S. H., Yang, M. S., and Park, C. M. (2011). Phenological growth stages of *Brachypodium distachyon*: codification and description. *Weed Res.* 51, 612–620. doi: 10.1111/j.1365-3180.2011.00877.x
- Howell, C. R., and Stipanovic, R. D. (1980). Suppression of *Pythium ultimum* induced damping-off of cotton seedlings by *Pseudomonas fluorescens* and its antibiotic pyoluteorin. *Phytopathology* 70, 712–715. doi: 10.1094/phyto-70-712
- Hummerjohann, J., Kuttel, E., Quadroni, M., Ragaller, J., Leisinger, T., and Kertesz, M. A. (1998). Regulation of the sulfate starvation response in *Pseudomonas aeruginosa*: role of cysteine biosynthetic intermediates. *Microbiology* 144, 1375–1386. doi: 10.1099/00221287-144-5-1375
- Kabbadj, A., Makoudi, B., Mouradi, M., Pauly, N., Frendo, P., and Ghoulam, C. (2017). Physiological and biochemical responses involved in water deficit tolerance of nitrogen-fixing *Vicia faba*. *PLoS One* 12:e0190284. doi: 10.1371/journal.pone.0190284
- Kamilova, F., Validov, S., Azarova, T., Mulders, I., and Lugtenberg, B. (2005). Enrichment for enhanced competitive plant root tip colonizers selects for a new class of biocontrol bacteria. *Environ. Microbiol.* 7, 1809–1817. doi: 10.1111/j.1462-2920.2005.00889.x
- Kanehisa, M., Araki, M., Goto, S., Hattori, M., Hirakawa, M., Itoh, M., et al. (2008). KEGG for linking genomes to life and the environment. *Nucleic Acids Res.* 36, D480–D484.
- Katoh, K., and Standley, D. M. (2013). MAFFT multiple sequence alignment software version 7: improvements in performance and usability. *Mol. Biol. Evol.* 30, 772–780. doi: 10.1093/molbev/mst010
- Kawasaki, A., Donn, S., Ryan, P. R., Mathiesin, U., Devilla, R., Jones, A., et al. (2016). Microbiome and exudates of the root and rhizosphere of *Brachypodium distachyon*, a model for wheat. *PLoS One* 11:e0164533. doi: 10.1371/journal.pone.0164533
- Kind, T., Wohlgemuth, G., Lee, D. Y., Lu, Y., Palazoglu, M., Shahbaz, S., et al. (2009). FiehnLib: mass spectral and retention index libraries for metabolomics based on quadrupole and time-of-flight gas chromatography/mass spectrometry. *Anal. Chem.* 81, 10038–10048. doi: 10.1021/ac9019522
- King, E. O., Ward, M. K., and Raney, D. E. (1954). Two simple media for the demonstration of pyocyanin and fluorescein. *J. Lab. Clin. Med.* 44, 301–307.
- Klonowska, A., Melkonian, R., Miche, L., Tisseyre, P., and Moulin, L. (2018). Transcriptomic profiling of *Burkholderia phyatum* STM815, *Cupriavidus taiwanensis* LMG19424 and *Rhizobium mesoamericanum* STM3625 in response to *Mimosa pudica* root exudates illuminates the molecular basis of their nodulation competitiveness and symbiotic evolutionary history. *BMC Genomics* 19:105. doi: 10.1186/s12864-018-4487-2
- Kobayashi, T., and Nishizawa, N. K. (2012). Iron uptake, translocation, and regulation in higher plants. *Annu. Rev. Plant Biol.* 63, 131–152. doi: 10.1146/annurev-arplant-042811-105522
- Kohler, P. R., Choong, E. L., and Rossbach, S. (2011). The RpiR-like repressor IolR regulates inositol catabolism in *Sinorhizobium meliloti*. *J. Bacteriol.* 193, 5155–5163. doi: 10.1128/jb.05371-11
- Lee, D., and Fiehn, O. (2008). High quality metabolomic data for *Chlamydomonas reinhardtii*. *Plant Meth.* 4:7. doi: 10.1186/1746-4811-4-7
- Letunic, I., and Bork, P. (2016). Interactive tree of life (iTOL) v3: an online tool for the display and annotation of phylogenetic and other trees. *Nucleic Acids Res.* 44, W242–W245.
- Li, L., Stoekert, C. J. Jr., and Roos, D. S. (2003). OrthoMCL: identification of ortholog groups for eukaryotic genomes. *Genome Res.* 13, 2178–2189. doi: 10.1101/gr.1224503
- Liao, Y., Smyth, G. K., and Shi, W. (2014). featureCounts: an efficient general purpose program for assigning sequence reads to genomic features. *Bioinformatics* 30, 923–930. doi: 10.1093/bioinformatics/btt656
- Liu, Y., Rainey, P. B., and Zhang, X. X. (2015). Molecular mechanisms of xylose utilization by *Pseudomonas fluorescens*: overlapping genetic responses to xylose, xylulose, ribose and mannitol. *Mol. Microbiol.* 98, 553–570. doi: 10.1111/mmi.13142
- Loper, J. E., Hassan, K. A., Mavrodi, D. V., Davis, E. W., Lim, C. K., Shaffer, B. T., et al. (2012). Comparative genomics of plant-associated *Pseudomonas* spp.: insights into diversity and inheritance of traits involved in multitrophic interactions. *PLoS Genet.* 8:e1002784. doi: 10.1371/journal.pgen.1002784
- Love, M. I., Huber, W., and Anders, S. (2014). Moderated estimation of fold change and dispersion for RNA-seq data with DESeq2. *Genome Biol.* 15:550.
- Lugtenberg, B., and Kamilova, F. (2009). Plant-growth-promoting rhizobacteria. *Annu. Rev. Microbiol.* 63, 541–556.
- Lugtenberg, B. J., Dekkers, L., and Bloemberg, G. V. (2001). Molecular determinants of rhizosphere colonization by *Pseudomonas*. *Annu. Rev. Phytopathol.* 39, 461–490.
- Lynch, J. M. (1990). “Microbial metabolites,” in *The Rhizosphere*, ed. J. M. Lynch (Chichester: John Wiley & Sons), 177–206.
- Mark, G. L., Dow, J. M., Kiely, P. D., Higgins, H., Haynes, J., Baysse, C., et al. (2005). Transcriptome profiling of bacterial responses to root exudates identifies genes involved in microbe-plant interactions. *Proc. Natl. Acad. Sci. U.S.A.* 102, 17454–17459. doi: 10.1073/pnas.0506407102
- Markowitz, V. M., Chen, I. M., Palaniappan, K., Chu, K., Szeto, E., Grechkin, Y., et al. (2012). IMG: the integrated microbial genomes database and comparative analysis system. *Nucleic Acids Res.* 40, D115–D122.
- Martinez-Gil, M., Yousef-Coronado, F., and Espinosa-Urgel, M. (2010). LapF, the second largest *Pseudomonas putida* protein, contributes to plant root colonization and determines biofilm architecture. *Mol. Microbiol.* 77, 549–561. doi: 10.1111/j.1365-2958.2010.07249.x
- Matilla, M. A., Espinosa-Urgel, M., Rodriguez-Herva, J. J., Ramos, J. L., and Ramos-Gonzalez, M. I. (2007). Genomic analysis reveals the major driving forces of bacterial life in the rhizosphere. *Genome Biol.* 8:R179.
- Miller, K. J., and Wood, J. M. (1996). Osmoadaptation by rhizosphere bacteria. *Annu. Rev. Microbiol.* 50, 101–136. doi: 10.1146/annurev.micro.50.1.101
- Moore, E. R. B., Tindall, B. J., Martins Dos Santos, V. A. P., Pieper, D. H., Ramos, J.-L., and Palleroni, N. J. (2006). “Nonmedical *Pseudomonas*,” in *The Prokaryotes*, eds M. Dworkin, S. Falkow, E. Rosenberg, K.-H. Schleifer, and E. Stackebrandt (New York, NY: Springer), 646–703.
- Mulet, M., Lalucat, J., and Garcia-Valdes, E. (2010). DNA sequence-based analysis of the *Pseudomonas* species. *Environ. Microbiol.* 12, 1513–1530.
- Naylor, D., DeGraaf, S., Purdom, E., and Coleman-Derr, D. (2017). Drought and host selection influence bacterial community dynamics in the grass root microbiome. *ISME J.* 11, 2691–2704. doi: 10.1038/ismej.2017.118
- Nguyen, C. (2003). Rhizodeposition of organic C by plants: mechanisms and controls. *Agronomie* 23, 375–396. doi: 10.1051/agro:2003011
- Nielsen, L., Li, X., and Halverson, L. J. (2011). Cell-cell and cell-surface interactions mediated by cellulose and a novel exopolysaccharide contribute to *Pseudomonas putida* biofilm formation and fitness under water-limiting conditions. *Environ. Microbiol.* 13, 1342–1356. doi: 10.1111/j.1462-2920.2011.02432.x
- Parejko, J. A., Mavrodi, D. V., Mavrodi, O. V., Weller, D. M., and Thomashow, L. S. (2012). Population structure and diversity of phenazine-1-carboxylic acid producing fluorescent *Pseudomonas* spp. from dryland cereal fields of central Washington state (USA) *Microb. Ecol.* 63, 226–241. doi: 10.1007/s00248-012-0015-0
- Phillips, D. A., Fox, T. C., King, M. D., Bhuvanewari, T. V., and Teuber, L. R. (2004). Microbial products trigger amino acid exudation from plant roots. *Plant Physiol.* 136, 2887–2894. doi: 10.1104/pp.104.044222
- Raaijmakers, J. M., Vandersluis, I., Koster, M., Bakker, P. A. H. M., Weisbeek, P. J., and Schippers, B. (1995). Utilization of heterologous siderophores and rhizosphere competence of fluorescent *Pseudomonas* spp. *Can. J. Microbiol.* 41, 126–135. doi: 10.1139/m95-017
- Raaijmakers, J. M., and Weller, D. M. (1998). Natural plant protection by 2,4-diacetylphloroglucinol-producing *Pseudomonas* spp. in take-all decline soils. *Mol. Plant Microbe Interact.* 11, 144–152. doi: 10.1094/mpmi.1998.11.2.144
- Rahman, M. M., Andberg, M., Thangaraj, S. K., Parkkinen, T., Penttila, M., Janis, J., et al. (2017). The crystal structure of a bacterial L-arabinonate dehydratase contains a [2Fe-2S] cluster. *ACS Chem. Biol.* 12, 1919–1927. doi: 10.1021/acschembio.7b00304
- Ramos-Gonzalez, M. I., Campos, M. J., and Ramos, J. L. (2005). Analysis of *Pseudomonas putida* KT2440 gene expression in the maize rhizosphere: *in vivo* expression technology capture and identification of root-activated promoters. *J. Bacteriol.* 187, 4033–4041. doi: 10.1128/jb.187.12.4033-4041.2005
- Reinhold-Hurek, B., Bunge, W., Burbano, C. S., Sabale, M., and Hurek, T. (2015). Roots shaping their microbiome: global hotspots for microbial activity. *Annu. Rev. Phytopathol.* 53, 403–424. doi: 10.1146/annurev-phyto-082712-102342

- Sanchez-Contreras, M., Martin, M., Villaceros, M., O'Gara, F., Bonilla, I., and Rivilla, R. (2002). Phenotypic selection and phase variation occur during alfalfa root colonization by *Pseudomonas fluorescens* F113. *J. Bacteriol.* 184, 1587–1596. doi: 10.1128/jb.184.6.1587-1596.2002
- Sarniguet, A., Kraus, J., Henkels, M. D., Muehlchen, A. M., and Loper, J. E. (1995). The sigma factor σ^s affects antibiotic production and biological control activity of *Pseudomonas fluorescens* Pf-5. *Proc. Natl. Acad. Sci. U.S.A.* 92, 12255–12259. doi: 10.1073/pnas.92.26.12255
- Schnider-Keel, U., Lejbolle, K. B., Baehler, E., Haas, D., and Keel, C. (2001). The sigma factor AlgU (AlgT) controls exopolysaccharide production and tolerance towards desiccation and osmotic stress in the biocontrol agent *Pseudomonas fluorescens* CHA0. *Appl. Environ. Microbiol.* 67, 5683–5693. doi: 10.1128/aem.67.12.5683-5693.2001
- Schroth, M. N., Hildebrand, D. C., and Panopoulos, N. J. (2006). “Phytopathogenic pseudomonads and related plant-associated pseudomonads,” in *The Prokaryotes*, eds M. Dworkin, S. Falkow, E. Rosenberg, K.-H. Schleifer, and E. Stackebrandt (New York, NY: Springer), 714–740. doi: 10.1007/0-387-30746-x_23
- Schwartz, C. J., Doyle, M. R., Manzaneda, A. J., Rey, P. J., Mitchell-Olds, T., and Amasino, R. M. (2010). Natural variation of flowering time and vernalization responsiveness in *Brachypodium distachyon*. *Bioenergy Res.* 3, 38–46. doi: 10.1007/s12155-009-9069-3
- Silby, M. W., Cerdano-Tarraga, A. M., Vernikov, G. S., Giddens, S. R., Jackson, R. W., Preston, G. M., et al. (2009). Genomic and genetic analyses of diversity and plant interactions of *Pseudomonas fluorescens*. *Genome Biol.* 10:R51.
- Silby, M. W., and Levy, S. B. (2004). Use of in vivo expression technology to identify genes important in growth and survival of *Pseudomonas fluorescens* Pf0-1 in soil: Discovery of expressed sequences with novel genetic organization. *J. Bacteriol.* 186, 7411–7419. doi: 10.1128/jb.186.21.7411-7419.2004
- Simons, M., Van Der Bij, A. J., Brand, I., De Weger, L. A., Wijffelman, C. A., and Lugtenberg, B. J. (1996). Gnotobiotic system for studying rhizosphere colonization by plant growth-promoting *Pseudomonas* bacteria. *Mol. Plant Microbe Interact.* 9, 600–607. doi: 10.1094/mpmi-9-0600
- Simons, M., Van Der Bij, A. J., Brand, J., De Weger, L. A., Wijffelman, D. A., and Lugtenberg, B. J. J. (1997). Amino acid synthesis is necessary for tomato root colonization by *Pseudomonas fluorescens* strain WCS365. *Mol. Plant Microbe Interact.* 10, 102–106. doi: 10.1094/mpmi.1997.10.1.102
- Smibert, R. M., and Kreig, N. R. (1994). “Phenotypic characterization,” in *Methods for General and Molecular Bacteriology*, eds P. Gerhardt, R. G. E. Murray, W. A. Wood, and N. R. Kreig (Washington, DC: American Society of Microbiology), 607–654.
- Thomashow, L. S., and Weller, D. M. (1988). Role of a phenazine antibiotic from *Pseudomonas fluorescens* in biological control of *Gaeumannomyces graminis* var. *tritici*. *J. Bacteriol.* 170, 3499–3508. doi: 10.1128/jb.170.8.3499-3508.1988
- Thomashow, L. S., Weller, D. M., Bonsall, R. F., and Pierson, L. S. (1990). Production of the antibiotic phenazine-1-carboxylic acid by fluorescent *Pseudomonas* species in the rhizosphere of wheat. *Appl. Environ. Microbiol.* 56, 908–912. doi: 10.1128/aem.56.4.908-912.1990
- Tyler, L., Fangel, J. U., Fagerstrom, A. D., Steinwand, M. A., Raab, T. K., Willats, W. G., et al. (2014). Selection and phenotypic characterization of a core collection of *Brachypodium distachyon* inbred lines. *BMC Plant Biol.* 14:25. doi: 10.1186/1471-2229-14-25
- Vacheron, J., Desbrosses, G., Bouffaud, M. L., Touraine, B., Moenne-Loccoz, Y., Muller, D., et al. (2013). Plant growth-promoting rhizobacteria and root system functioning. *Front. Plant Sci.* 4:356. doi: 10.3389/fpls.2013.00356
- van den Broek, D., Bloembergen, G. V., and Lugtenberg, B. (2005). The role of phenotypic variation in rhizosphere *Pseudomonas* bacteria. *Environ. Microbiol.* 7, 1686–1697. doi: 10.1111/j.1462-2920.2005.00912.x
- van Veen, J. A., Van Overbeek, L. S., and Van Elsas, J. D. (1997). Fate and activity of microorganisms introduced into soil. *Microbiol. Mol. Biol. Rev.* 61, 121–135. doi: 10.1128/61.2.121-135.1997
- Walker, T. S., Bais, H. P., Halligan, K. M., Stermitz, F. R., and Vivanco, J. M. (2003). Metabolic profiling of root exudates of *Arabidopsis thaliana*. *J. Agric. Food Chem.* 51, 2548–2554.
- Wargo, M. J. (2013a). Choline catabolism to glycine betaine contributes to *Pseudomonas aeruginosa* survival during murine lung infection. *PLoS One* 8:e56850. doi: 10.1371/journal.pone.0056850
- Wargo, M. J. (2013b). Homeostasis and catabolism of choline and glycine betaine: lessons from *Pseudomonas aeruginosa*. *Appl. Environ. Microbiol.* 79, 2112–2120.
- Whipps, J. M. (1990). “Carbon economy,” in *The Rhizosphere*, ed. J. M. Lynch (Chichester: John Wiley & Sons), 59–97.
- Winsor, G. L., Van Rossum, T., Lo, R., Khaira, B., Whiteside, M. D., Hancock, R. E., et al. (2009). *Pseudomonas Genome Database*: facilitating user-friendly, comprehensive comparisons of microbial genomes. *Nucleic Acids Res.* 37, D483–D488.
- Yahr, T. L., and Parsek, M. R. (2006). “*Pseudomonas aeruginosa*,” in *The Prokaryotes*, eds M. Dworkin, S. Falkow, E. Rosenberg, K.-H. Schleifer, and E. Stackebrandt (New York, NY: Springer), 704–713.
- Yancey, P. H., Clark, M. E., Hand, S. C., Bowlus, R. D., and Somero, G. N. (1982). Living with water stress: evolution of osmolyte systems. *Science* 217, 1214–1222.
- Ye, J., Zhang, Y., Cui, H., Liu, J., Wu, Y., Cheng, Y., et al. (2018). WEGO 2.0: a web tool for analyzing and plotting GO annotations, 2018 update. *Nucleic Acids Res.* 46, W71–W75.
- Yoshida, K., Yamaguchi, M., Morinaga, T., Kinehara, M., Ikeuchi, M., Ashida, H., et al. (2008). myo-Inositol catabolism in *Bacillus subtilis*. *J. Biol. Chem.* 283, 10415–10424.
- Yousef-Coronado, F., Travieso, M. L., and Espinosa-Urgel, M. (2008). Different, overlapping mechanisms for colonization of abiotic and plant surfaces by *Pseudomonas putida*. *FEMS Microbiol. Lett.* 288, 118–124.
- Zboralski, A., and Filion, M. (2020). Genetic factors involved in rhizosphere colonization by phytobeneficial *Pseudomonas* spp. *Comput. Struct. Biotechnol. J.* 18, 3539–3554.
- Zolla, G., Bakker, M. G., Badri, D. V., Chaparro, J. M., Sheflin, A. M., Manter, D. K., et al. (2013). “Understanding root-microbiome interactions,” in *Molecular Microbial Ecology of the Rhizosphere*, ed. F. J. De Bruijn (Hoboken, NJ: John Wiley & Sons), 745–754.

Conflict of Interest: The authors declare that the research was conducted in the absence of any commercial or financial relationships that could be construed as a potential conflict of interest.

Copyright © 2021 Mavrodi, McWilliams, Peter, Berim, Hassan, Elbourne, LeTourneau, Gang, Paulsen, Weller, Thomashow, Flynt and Mavrodi. This is an open-access article distributed under the terms of the Creative Commons Attribution License (CC BY). The use, distribution or reproduction in other forums is permitted, provided the original author(s) and the copyright owner(s) are credited and that the original publication in this journal is cited, in accordance with accepted academic practice. No use, distribution or reproduction is permitted which does not comply with these terms.